A&A manuscript no.
(will be inserted by hand later)

Your thesaurus codes are:
(12.03.4; 12.04.1; 12.12.1; Universe 11.03.1;

ASTRONOMY
AND
ASTROPHYSICS
1.2.2008

arXiv:astro-ph/9912511v3 16 Feb 2000

Cosmological parameters from large scale structure observations

B. Novosyadlyj[1], R. Durrer[2], S. Gottlöber[3], V.N. Lukash[4], S. Apunevych[1]

[1] Astronomical Observatory of L'viv State University, Kyryla and Mephodia str.8, 290005, L'viv, Ukraine
[2] Department de Physique Théorique, Université de Genève, Quai Ernest Ansermet 24, CH-1211 Genève 4, Switzerland
[3] Astrophysikalisches Institut Potsdam, An der Sternwarte 16, D-14482 Potsdam, Germany
[4] Astro Space Center of Lebedev Physical Institute of RAS, Profsoyuznaya 84/32, 117810 Moscow, Russia

Received ...; accepted ...

Abstract. The possibility of determining cosmological parameters on the basis of a wide set of observational data including the Abell-ACO cluster power spectrum and mass function, peculiar velocities of galaxies, the distribution of Ly-α clouds and CMB temperature fluctuations is analyzed. Using a χ^2 minimization method, assuming $\Omega_\Lambda + \Omega_{\rm matter} = 1$ and no contribution from gravity waves, we show that this data set determines quite precisely the values of the spectral index n of the primordial power spectrum, baryon, cold dark matter and massive neutrino density Ω_b, Ω_{cdm} and Ω_ν respectively, the Hubble constant $h \equiv H_0/(100{\rm km/s/Mpc})$ and the value of the cosmological constant, Ω_Λ .

Varying all parameters, we found that a tilted ΛMDM model with one sort of massive neutrinos and the parameters $n = 1.12 \pm 0.10$, $\Omega_m = 0.41 \pm 0.11$ ($\Omega_\Lambda = 0.59 \pm 0.11$), $\Omega_{cdm} = 0.31 \pm 0.15$, $\Omega_\nu = 0.059 \pm 0.028$, $\Omega_b = 0.039 \pm 0.014$ and $h = 0.70 \pm 0.12$ matches observational data best.

Ω_ν is higher for more species of massive neutrinos, ~ 0.1 for two and ~ 0.13 for three species. Ω_m raises by ~ 0.08 and ~ 0.15 respectively.

The 1σ (68.3%) confidence limits on each cosmological parameter, which are obtained by marginalizing over the other parameters, are $0.82 \le n \le 1.39$, $0.19 \le \Omega_m \le 1$ ($0 \le \Omega_\Lambda \le 0.81$), $0 \le \Omega_\nu \le 0.17$, $0.021 \le \Omega_b \le 0.13$ and $0.38 \le h \le 0.85$ $1.5 \le b_{cl} \le 3.5$. Here b_{cl} is the cluster bias parameter. The best-fit parameters for 31 models which are inside of 1σ range of the best model are presented (Table 4).

Varying only a subset of parameters and fixing the others changes the results. In particular, if a pure matter model ($\Omega_m = 1$) is assumed, MDM with $\Omega_\nu = 0.22 \pm 0.08$, three species of massive neutrinos and low $h = 0.47 \pm 0.05$ matches the observational data best. If a low density Universe $\Omega_m = 0.3$ is assumed, a ΛCDM model without hot dark matter and high $h = 0.71$ matches the observational data best. If the primordial power spectrum is scale invariant ($n \equiv 1$) a low density Universe ($\Omega_m = 0.45 \pm 0.12$, $h = 0.71 \pm 0.13$) with very little hot dark matter ($\Omega_\nu = 0.04 \pm 0.03$, $N_\nu = 1$) becomes the best fit.

It is shown also that observational data set used here rules out the class of CDM models with $h \ge 0.5$, scale invariant primordial power spectrum, zero cosmological constant and spatial curvature at very high confidence level, $> 99.99\%$. The corresponding class of MDM models are ruled out at $\sim 95\%$ C.L.

Key words: Large Scale Structure: cosmological models, power spectrum, cosmological parameters

1. Introduction

Observations of the large scale structure (LSS) of the Universe carried out during the last years and coming up from current experiments and observational programs allow to determine the parameters of cosmological models and the nature of dark matter more precisely. The usual cosmological paradigm - a scale free power spectrum of scalar primordial perturbations which evolve in a multicomponent medium to form the large scale structure of the Universe - is compatible with the observed cosmic microwave background (CMB) temperature fluctuations. Most inflationary scenarios predict a scale free primordial power spectra of scalar density fluctuations $P(k) \sim k^n$ with arbitrary n as well as gravity waves which contribute to the power spectrum of CMB temperature fluctuations $(\frac{\Delta T}{T})_\ell$ at low spherical harmonics. But models with a minimal number of free parameters, such as the scale invariant ($n = 1$) standard cold dark matter model (SCDM) or the standard mixed (cold plus hot) dark matter model (SMDM)

Send offprint requests to: Bohdan Novosyadlyj

only marginally match observational data. Better agreement between predictions and observational data can be achieved in models with a larger number of parameters: cold dark matter (CDM) or mixed dark matter (MDM) with baryons, a tilted primordial power spectra, spatial curvature (Ω_k), a cosmological constant (Ω_Λ) and a tensor contribution to the CMB anisotropy power spectrum.

The neutrino oscillations discovered recently in the Super-Kamiokande experiment (Fukuda et al. 1998) show that at least one species of weakly interacting neutrinos have non-zero rest mass. Assuming that the larger one of them is about $m_\nu \simeq \sqrt{\delta m_\nu^2} \approx 0.07$ eV we find $\Omega_\nu \approx 7.4 \times 10^{-4} N_\nu / h^2$. It is also possible that one, two or three species have masses in the eV range and give appreciable contribution to the dark matter content of the Universe.

The presence of rich clusters of galaxies at $z \approx 0.54$, 0.55, 0.8 (Bahcall & Fan 1998) indicates a low matter density.

In this work we do not include into our analysis the recent observations of distant supernovae (Perlmutter et al. 1998, Riess et al. 1998). The SNeIa measurements support a positive cosmological constant. Assuming a flat Universe, $\Omega_\Lambda + \Omega_m = 1$, a value of $\Omega_\Lambda \sim 0.7$ is preferred (see also the review by Bahcall et al. 1999), but, in agreement with Valdarnini et al. 1998, Primack & Gross 1998, we find that on the basis of LSS data alone, a non-vanishing cosmological constant is preferred within the class of models analyzed in this work.

Another approach based on the search of best-fit cosmological parameters in open and critical density CDM and ΛCDM models without gravitational waves for the total combination of observational data on CMB anisotropy has been carried out by Lineweaver & Barbosa 1998. But the CMB data set corresponds to very large scales ($\geq 100 h^{-1}$Mpc) and it is not sufficiently sensitive to the existence of a HDM component. The power spectra of density fluctuations obtained from the spatial distribution of Abell-ACO clusters (Einasto et al. 1997, Retzlaff et al. 1998), APM, CfA and IRAS galaxy surveys (Einasto et al. 1999 and references therein) are extended to smaller scales up to galaxy scales which are below the neutrino free streaming scale. On small scales constraints are obtained from absorption features in quasar spectra known as the Ly-α forest (Gnedin 1998, Croft et al. 1998).

The determination of cosmological parameters from some observations of the LSS of the Universe was carried out in many papers (e.g. Atrio-Barandela et al. 1997, Lineweaver & Barbosa 1998, Tegmark 1999, Bridle et al. 1999, Novosyadlyj 1999 and references therein). Recently, Bridle et al. 1999 have analyzed the cluster abundances, CMB anisotropies and IRAS observations to optimize the four parameters (Ω_m, h, σ_8, and $b_{\rm IRAS}$ in a open CDM model. Atrio-Barandela et al. 1997 use the cluster power spectrum together with data of the Saskatoon experiment to discuss the possible existence of a built-in scale in the primordial power spectrum. In this paper a total of 23 measurements from sub-galaxy scales (Ly-α clouds) over cluster scales up to the horizon scale (CMB quadrupole) are used to determine seven cosmological parameters.

Clearly, it is possible that the 'correct cosmological model' is not one of those analyzed in this paper. If the data are good enough this can in principle be decided by a χ^2-test. As long as we find a model within the family of models studied here with an acceptable value of χ^2, we have no compelling reason to consider other models.

In view of the growing body of observational data, we want to discuss the quantitative differences between theory and observations for the entire class of available models by varying all the input parameters such as the tilt of the primordial spectrum, n, the density of cold dark matter, Ω_{cdm}, hot dark matter, Ω_ν, and baryons, Ω_b, the vacuum energy or cosmological constant, Ω_Λ, and the Hubble parameter h, to find the values which agree best with observations of LSS on all scales (or even to exclude a whole family of models). Here we restrict ourselves to the analysis of spatially flat cosmological models with $\Omega_\Lambda + \Omega_m = 1$ ($\Omega_k = 0$), where $\Omega_m = \Omega_{cdm} + \Omega_b + \Omega_\nu$, and to an inflationary scenario without tensor mode. We also neglect the effect of a possible early reionization which could reduce the amplitude of the first acoustic peak in the CMB anisotropy spectrum.

The reason for the restriction of flat models is mainly numerical. However, the new CMB anisotropy data from the Boomerang experiment actually strongly favors spatially flat universes (Melchiorri et al. 1999b). Neglecting the tensor mode which affects the normalization and the height of the first acoustic peak is motivated by the work of Tegmark 1999, who found that CMB anisotropy data prefer no or a small tensor component, however there are also arguments in favor of the importance of the tensor mode (Arkhipova et al. 1998, Melchiorri et al. 1999a). Furthermore, since the LSS data used in this paper disfavors very blue spectra, the high acoustic peak indicates that reionization cannot be substantial for the class of models analyzed in this paper. Hence we set the optical depth $\tau = 0$.

The outline of this paper is as follows: In Sect. 2 we describe the observational data which are used. The method of parameter determination and some tests are described in Sect. 3. We present the results obtained under different assumptions about the parameter ranges in Sect. 4. A discussion of our results and the conclusions are given in Sects. 5 and 6 respectively.

2. The experimental data set

2.1. The Abell-ACO cluster power spectrum

One might expect that the most favorable data for the determination of cosmological parameters are power spec-

tra constructed from the observed distribution of galaxies. But the power spectra of galaxies obtained from the two-dimensional APM survey (e.g. Maddox et al. 1996, Tadros & Estathiou 1996, and references therein), the CfA redshift survey (Vogeley et al. 1992, Park et al. 1994), the IRAS survey (Saunders et al. 1992) and/or from the Las Campanas Redshift Survey (da Costa et al. 1994, Landy et al. 1996) differ both in the amplitude and in the behavior near the maximum. Moreover, nonlinear effects on small scale must be taken into account in their analysis. For these reasons we do not include galaxy power spectra for the determination of parameters in this work. Here, we use the power spectrum of Abell-ACO clusters (Einasto et al. 1997, Retzlaff et al. 1998) as observational input. This power spectrum is measured in the range $0.03h/\mathrm{Mpc} \leq k \leq 0.2h/\mathrm{Mpc}$. The cluster power spectrum is biased with respect to the dark matter distribution. We assume that the bias is linear and scale independent in the range of scales considered. The position of the maximum ($k_{max} \approx 0.05h/\mathrm{Mpc}$) and the slope at lower and larger scales are sensitive to the baryon content Ω_b, the Hubble constant h, the neutrino mass m_ν and the number of species of massive neutrinos N_ν (Novosyadlyj 1999). The Abell-ACO cluster power spectrum $\tilde{P}_{A+ACO}(k_j)$ (here and in the following a tilde denotes observed quantities) has been taken from Retzlaff et al. 1998. We present 13 values of $\tilde{P}_{A+ACO}(k_j)$ and the 1σ errors in Table 1 and in Fig. 1. In a first step, we have assumed that the 13 points in this power spectrum given below are independent measurements. The value of χ^2 obtained under this assumption is much smaller than the number of degrees of freedom (see below). We interpret this as a hint that the 13 points of $\tilde{P}_{A+ACO}$ given in Table I cannot be considered as independent measurements. We therefore describe the power spectrum by three parameters A, $k_{\rm bend}$ and α to be of the form

$$\tilde{P}_{A+ACO}(k) = \frac{Ak}{1+(k/k_{\rm bend})^\alpha} \ . \qquad (1)$$

A fit of the parameters to the observed power spectrum gives

$$A = (3.78 \pm 1.71) \times 10^6, \quad k_{\rm bend} = 0.056 \pm 0.015,$$

$$\alpha = 3.49 \pm 0.72. \qquad (2)$$

In Fig. 1 we show the observed power spectrum together with the fit. The cosmological model parameters obtained using the full power spectrum information or the three parameter fit are in good agreement, but the latter prescription leads to a more reasonable value of χ^2.

This point is quite important since it illustrates that a small χ^2 need not mean that the error bars of the data are too large but it can be due to data points depending only on a few parameters and therefore not being independent. If a power spectrum, like the one above can be modeled by 3 parameters, then, by varying three cosmological parameters, like *e.g.* the cluster bias b_c , the HDM contribution Ω_ν and the Hubble parameter, h, we can in general (if there is no degeneracy) fit all three parameters A, $k_{\rm bend}$ and α and thereby the entire power spectrum. The number of degrees of freedom in such a fit is 0 and not 10 as one would infer form the number points of the power spectrum.

To make best use of the observational information, we nevertheless use the full 13 points of the power spectrum to fit the data, but we assign it $n_F = 3$ for the number of degrees of freedom.

Table 1. The Abell-ACO power spectrum by Retzlaff et al. 1998

No	k_j	$\tilde{P}_{A+ACO}(k_j) \pm \Delta\tilde{P}$
1	0.030	$(9.31 \pm 5.97) \cdot 10^4$
2	0.035	$(1.04 \pm 0.66) \cdot 10^5$
3	0.040	$(1.04 \pm 0.58) \cdot 10^5$
4	0.047	$(1.26 \pm 0.51) \cdot 10^5$
5	0.054	$(1.45 \pm 0.69) \cdot 10^5$
6	0.062	$(1.02 \pm 0.39) \cdot 10^5$
7	0.072	$(8.10 \pm 2.52) \cdot 10^4$
8	0.083	$(5.44 \pm 2.19) \cdot 10^4$
0	0.096	$(5.30 \pm 2.49) \cdot 10^4$
10	0.11	$(3.85 \pm 1.33) \cdot 10^4$
11	0.13	$(2.03 \pm 0.86) \cdot 10^4$
12	0.15	$(2.04 \pm 0.98) \cdot 10^4$
13	0.17	$(1.70 \pm 0.94) \cdot 10^4$

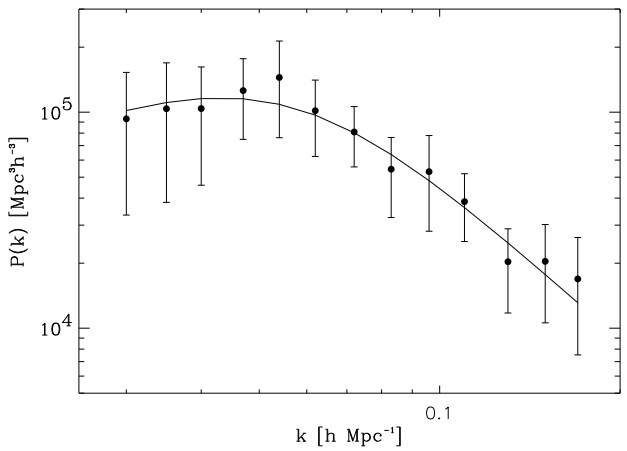

Fig. 1. The Abell-ACO power spectrum by Retzlaff et al. 1998. The solid line is the best fit according to Eqs. 1 and 2.

2.2. CMB data

We normalize the power spectrum using the COBE 4-year data of CMB temperature fluctuations (Bennett et al. 1996, Liddle et al. 1996, Bunn and White 1997). We believe that using all available experimental data on $\Delta T/T$ on angular scales smaller than the COBE measurement is not an optimal way for searching of best-fit parameters because some data points in CMB spectrum contradict each other. Therefore, we use only the position and amplitude of the first acoustic peak derived from observational data as integral characteristics of CMB power spectrum, which are sensitive to some of the model parameters.

To determine the position, ℓ_p, and amplitude, A_p, of the first acoustic peak we use the set of observational data on CMB temperature anisotropy given in Table 2 (altogether 51 observational points). For each experiment we include the effective harmonic, the amplitude of the temperature fluctuation at this harmonic, the upper and lower error in the temperature, and the effective range of the window in ℓ-space. In those cases when original papers do not contain effective harmonics and band width we have taken them from Max Tegmark's CMB data analysis center (Tegmark 1999) dated Nov 25 1999. We fit the experimental data points by a polynomial of 6-th order using the Levenberg-Marquardt method to determine the position and amplitude of the first peak: $[l(l+1)C_l/2\pi^2]^{1/2} = \sum_{i=0}^{6} a_i l^i$. The best-fit values of the coefficients are: $a_0 = 31.1$, $a_1 = -0.309$, $a_2 = 5.18 \times 10^{-3}$, $a_3 = 9.66 \times 10^{-6}$, $a_4 = -3.68 \times 10^{-8}$, $a_5 = 1.22 \times 10^{-10}$, $a_6 = -9.19 \times 10^{-14}$ ($\chi^2 = 62.9$). The amplitude A_p and position l_p of first acoustic peak determined from data fitting curve are 79.6μK and 253 correspondingly. Our result differs only slightly from the numbers obtained by Lineweaver & Barbosa 1998 who found 260 and 88μK. Fig. 2 shows the observational data used together with the polynomial best fit (solid line).

We estimated the error of A_p and l_p in the following way.

By varying of all coefficients a_i we determine χ^2-hyper-surface in 7-dimension parameter space which contains deviations of less than 1σ. If the probability distribution obeys Gaussian statistics, this corresponds to a 68.3% confidence level. It is well known, that present CMB anisotropy data even on small scales do not obey Gaussian statistics and thus this procedure is somewhat arbitrary. However, it can be assumed that this gives us a good indication for the errors bar in position and amplitude of the first acoustic peak. For 44 degrees of freedom (51 data points minus 7 parameters) this hyper-surface corresponds to $\Delta\chi^2 = 47.9$. For values of parameters a_i which have a $\chi^2 < \chi^2_{min} + \Delta\chi^2$ we calculate the C_l's and find the peak amplitude A_p and the position l_p. They are in the contour line in the $A_p - l_p$ plane shown in Fig. 3. The upper-lower and right-left extremal points indicate 1σ statistical errors: $\Delta A_p^{st} = +17.0, -16.3\mu$K and $\Delta l_p^{st} = +28, -22$. Uncertainties of effective harmonics of each experiment do not influence the error of the amplitude of the first acoustic peak but must be take into account for the full error in the peak position, so that $\Delta l_p = \Delta l_p^{st} + \Delta l_p^{w}$, where last term is the mean band width around l_p. We estimate it as mean width of all experiments weighted by acoustic peak amplitude $\Delta l_p^{w} = \sum_{i=1}^{56} (\Delta l)_i \omega_i / \sum_{i=1}^{56} \omega_i$, where the weighting factor $\omega_i = [l_i(l_i+1)C_{l_i}/2\pi^2]^{1/2}/A_p$ is calculated using polynomial fit. This finally leads to $\Delta l_p^{w} \approx 45.0$. (Without weighting the value is $\Delta l_p^{w} \approx 42$). Therefore, the errors of determination of first acoustic peak amplitude and position are $\Delta A_p \approx 16.5\mu$K and $\Delta l_p \approx 70$ respectively. We use these errors below in our search of cosmological parameters.

It is interesting to note that no 6th order polynomial fits the data really well. For our best fit polynomial we obtain $\chi^2 = 62.9$ for 51 data points and 7 parameters. The probability for this polynomial leading to the observed data is about 1%. This big χ^2 can have two origins. First, the probability distribution is non-Gaussian and, therefore, the probability to obtain this value of χ^2 is higher than 1%. Secondly, some data seems to be contradictory. For example, if we ignore all the Python V points we obtain a best fit polynomial with $\chi^2 = 23$ which is even slightly too low. (Removing of these points does not change essentially the result amplitude and position of acoustic peak, $\ell_p = 256$, $A_p = 79.0$ without them). But of course we are not allowed without any good reason, to leave away some experimental results. It may well be that Python V is correct and some other experiments are wrong. Therefore, we adopted this somewhat hand waving way to extract information from this data. Clearly, a more thorough analysis with true, non-Gaussian likelihood functions would be in order, which we leave for the future (see Bartlett et al. 1999).

For the comparison of models with the CMB data we use, apart from the COBE normalization, only the two parameters obtained by the fitting procedure described above: the effective harmonic $\ell_p = 253 \pm 70$ of the peak position and the amplitude of the peak $A_p = 79.6 \pm 16.5\mu$K. Clearly, this position and height of the first acoustic peak is not strictly implied by the present data and can therefore be criticized. In this sense it has to be considered primarily as a working hypothesis which will be confirmed or contradicted in the future by more accurate data.

2.3. Other experimental constraints

A constraint of the amplitude of the fluctuation power spectrum at cluster scale can be derived from the cluster mass and the X-ray temperature functions. It is usually formulated as a constraint for the density fluctuation in

Table 2. Observational data on CMB temperature fluctuations (in μK)

$\ell_{\rm min}$	$\ell_{\rm eff}$	$\ell_{\rm max}$	$\delta T^{obs}_{\ell_{\rm eff}}$	$+err$	$-err$	Experiment
2.5	**3.1**	3.7	**28.0**	+7.5	−10.3	COBE2, Tegmark & Hamilton 1997
3.4	**4.1**	4.8	**34.0**	+6.0	−7.2	COBE3, Tegmark & Hamilton 1997
4.7	**5.6**	6.5	**25.1**	+5.3	−6.6	COBE4, Tegmark & Hamilton 1997
6.7	**8**	9.3	**29.4**	+3.6	−4.1	COBE5, Tegmark & Hamilton 1997
2	**10**	28	**29.4**	+7.8	−7.7	FIRS, Ganga et al. 1994 *)
9.6	**10.9**	12.2	**27.7**	+3.9	−4.5	COBE6, Tegmark & Hamilton 1997
11.8	**14.3**	16.8	**26.1**	+4.4	−5.2	COBE7, Tegmark & Hamilton 1997
16.6	**19.4**	22.2	**33.0**	+4.6	−5.4	COBE8, Tegmark & Hamilton 1997
12	**20**	30	**32.5**	+10.1	−8.5	Tenerife, Hancock et al. 1997 *)
21	**50**	94	**23.0**	+3.0	−3.0	PythonV1, Coble et al. 1999
40	**53**	75	**54.5**	+27.2	−22.0	iac/bartol2, Femenia et al. 1997
36	**68**	106	**30.2**	+24.8	−17.4	SP91, Gundersen et al. 1995
36	**68**	106	**36.3**	+34.3	−20.0	SP94, Gundersen et al. 1995
25	**58**	75	**29.0**	+30.0	−23.2	Boomerang, Mauskopf et al. 1999
28	**74**	97	**55.6**	+29.6	−15.2	BAM, Tucker et al. 1997 *)
35	**74**	130	**26.0**	+4.0	−4.0	PythonV2, Coble et al. 1999
39	**80**	121	**47.0**	+6.0	−7.0	QMap F1+2Ka, de Oliveira-Costa et al. 1998
39	**84**	130	**35.0**	+15.0	−11.0	MSAM, Wilson et al. 1999
58	**87**	126	**49.0**	+8.0	−5.0	SK1, Netterfield et al. 1997
68	**92**	129	**54.0**	+14.0	−12.0	Python1, Platt et al. 1997
51	**95**	173	**39.1**	+8.7	−8.7	Argo1, de Bernardis et al. 1994 *)
51	**95**	173	**46.8**	+9.5	−12.1	Argo2, Masi et al. 1996 *)
76	**102**	125	**48.8**	+31.5	−27.9	Boomerang, Mauskopf et al. 1999
67	**108**	157	**31.0**	+5.0	−4.0	PythonV3, Coble et al. 1999
47	**111**	175	**52.0**	+5.0	−5.0	QMap F1+2Q, de Oliveira-Costa et al. 1998
65	**120**	221	**94.5**	+41.8	−41.8	IAB, Piccirillio et al. 1993 *)
72	**126**	180	**59.0**	+6.0	−7.0	QMap F1+2Ka, de Oliveira-Costa et al. 1998
95	**128**	154	**55.0**	+18.0	−17.0	TOCO98, Miller et al. 1999
72	**139**	247	**49.4**	+7.8	−7.8	MAX, Tanaka et al. 1996 *)
99	**140**	185	**28.0**	+8.0	−9.0	PythonV4, Coble et al. 1999
114	**152**	178	**82.0**	+11.0	−11.0	TOCO98, Miller et al. 1999
126	**153**	175	**67.0**	+37.1	−33.8	Boomerang, Mauskopf et al. 1999
123	**166**	209	**69.0**	+7.0	−6.0	SK2, Netterfield et al. 1997
119	**177**	243	**58.0**	+15.0	−13.0	Python2, Platt et al. 1997
132	**172**	215	**54.0**	+10.0	−11.0	PythonV5, Coble et al. 1999
131	**201**	283	**49.0**	+10.0	−8.0	MSAM, Wilson et al. 1999
164	**203**	244	**96.0**	+15.0	−15.0	PythonV6, Coble et al. 1999
176	**204**	225	**71.9**	+38.7	−36.3	Boomerang, Mauskopf et al. 1999
170	**226**	263	**83.0**	+7.0	−8.0	TOCO98, Miller et al. 1999
195	**233**	273	**91.0**	+32.0	−38.0	PythonV7, Coble et al. 1999
196	**237**	266	**85.0**	+10.0	−8.0	Sk3, Netterfield et al. 1997
226	**255**	275	**61.0**	+38.7	−36.1	Boomerang, Mauskopf et al. 1999
248	**286**	310	**86.0**	+12.0	−10.0	SK4, Netterfield et al. 1997
276	**305**	325	**55.0**	+40.9	−39.1	Boomerang, Mauskopf et al. 1999
247	**306**	350	**70.0**	+10.0	−11.0	TOCO98, Miller et al. 1999
308	**349**	393	**69.0**	+19.0	−28.0	SK5, Netterfield et al. 1997
332	**397**	481	**50.8**	+15.4	−15.4	CAT1, Scott et al. 1996 *)
326	**403**	475	**32.0**	+31.9	−30.0	Boomerang, Mauskopf et al. 1999
284	**407**	453	**47.0**	+7.0	−8.0	MSAM, Wilson et al. 1999
361	**589**	756	**56.0**	+8.1	−6.9	Ring5M2, Leitch et al. 1998
543	**615**	717	**49.0**	+19.1	−13.6	CAT2, Scott et al. 1996 *)

*) - ℓ_{eff} and band width were taken from Max Tegmark's CMB data analysis center (Tegmark 1999)

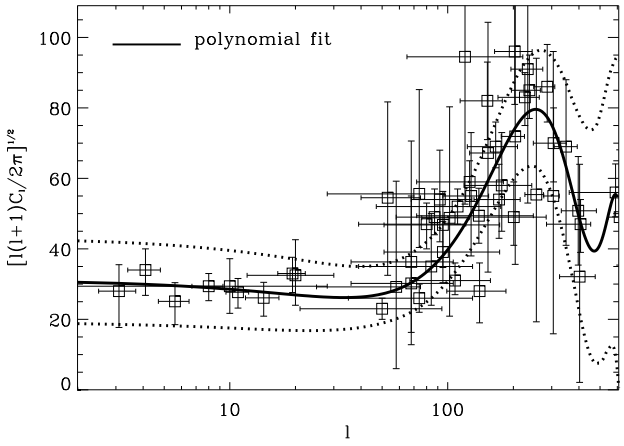

Fig. 2. Observational data of CMB fluctuation (Table 2) and a sixth order polynomial fit to a power spectrum (solid line). The dotted lines restrict the space of fitting curves which deviate from best fit by less than 1σ ($\Delta\chi^2 = 47.9$ for 44 degrees of freedom).

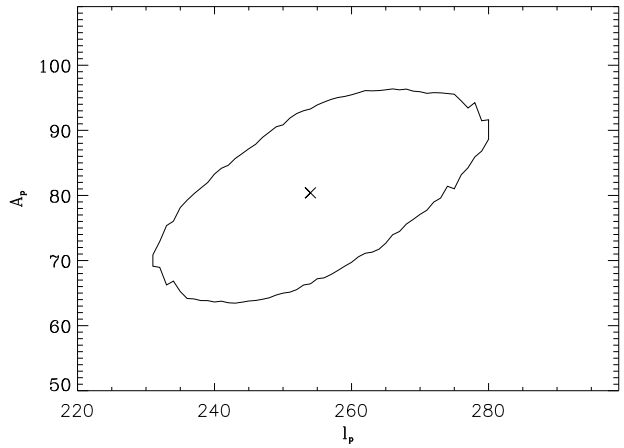

Fig. 3. The contour of positions l_p and amplitudes A_p of first acoustic peak which corresponds to the range of fitting curves which are in the 68.3% range of probability of point distribution. The box which contains ellipse gives 1σ errors for l_p and A_p. The position l_p and amplitude A_p for best fit coefficients are shown as a cross (see also in Fig. 2).

a top-hat sphere of $8h^{-1}$ Mpc radius, σ_8, which can be calculated for a given initial power spectrum $P(k)$:

$$\sigma_8^2 = \frac{1}{2\pi^2}\int_0^\infty k^2 P(k) W^2(8\mathrm{Mpc}\ k/h)dk, \qquad (3)$$

where $W(x) = 3(\sin x - x\cos x)/x^3$ is the Fourier transform of a top-hat window function. A recent optical determination of the mass function of nearby galaxy clusters (Girardi et al. 1998) gives $\tilde{\sigma}_8\tilde{\Omega}_m^{0.46-0.09\Omega_m} = 0.60 \pm 0.04$. Several groups have found similar results using different methods and different data sets (for a comprehensive list of references see Borgani et al. 1999). To take into account the results from other authors we have decided to use more conservative error bars:

$$\tilde{\sigma}_8\tilde{\Omega}_m^{0.46-0.09\Omega_m} = 0.60 \pm 0.08\ . \qquad (4)$$

¿From the existence of three very massive clusters of galaxies observed so far at $z > 0.5$ a further constraint has been established by Bahcall & Fan 1998

$$\tilde{\sigma}_8\tilde{\Omega}_m^{\alpha} = 0.8 \pm 0.1\ , \qquad (5)$$

where $\alpha = 0.24$ if $\Omega_\Lambda = 0$ and $\alpha = 0.29$ if $\Omega_\Lambda > 0$ with $\Omega_\Lambda + \Omega_m = 1$. The relation of this value to other tests will be analyzed too.

Another constraint on the amplitude of the linear power spectrum of density fluctuations in our vicinity comes from the study of galaxy bulk flows in spheres of large enough radius around our position. Since these data may be influenced by the local super-cluster (cosmic variance), we will use only the value of bulk motion - the mean peculiar velocity of galaxies in the sphere of radius $50h^{-1}$Mpc given by Kolatt & Dekel 1997,

$$\tilde{V}_{50} = (375 \pm 85)\mathrm{km/s}. \qquad (6)$$

An essential constraint on the linear power spectrum of matter clustering on small scales ($k \sim (2-40)h$/Mpc comes from the Ly-α forest of absorption lines seen in quasar spectra (Gnedin 1998, Croft et al. 1998 and references therein). Assuming that the Ly-α forest is formed by discrete clouds with a physical size close to the Jeans scale in the reionized inter-galactic medium at $z \sim 2-4$, Gnedin 1998 has obtained a constraint on the value of the r.m.s. linear density fluctuations

$$1.6 < \tilde{\sigma}_F(z=3) < 2.6\ \ (95\%\mathrm{C.L.}) \qquad (7)$$
$$\text{at}\ \ k_F \approx 34\Omega_m^{1/2} h/\mathrm{Mpc}\ .$$

Taking into account the new data on quasar absorption lines, the effective equation of state and the temperature of the inter-galactic medium at high redshift were re-estimated recently by Ricotti et al. 1999. As result the value of Jeans scale at $z = 3$ has moved to $k_F \approx 38\Omega_m^{1/2} h/\mathrm{Mpc}$ (Gnedin 1999).

The procedure of recovering the linear power spectrum from the Ly-α forest has been elaborated by Croft et al. 1998. Analyzing the absorption lines in a sample of 19 QSO spectra they have obtained the following constraint on the amplitude and slope of the linear power spectrum at $z = 2.5$ and $k_p = 1.5\Omega_m^{1/2} h/\mathrm{Mpc}$,

$$\tilde{\Delta}_\rho^2(k_p) \equiv k_p^3 P(k_p)/2\pi^2 = 0.57 \pm 0.26, \qquad (8)$$

$$\tilde{n}_p \equiv \frac{\Delta \log\ P(k)}{\Delta \log\ k}\ |_{k_p} = -2.25 \pm 0.18, \qquad (9)$$

(95% CL). In addition to the power spectrum measurements we will use the constraints on the value of the Hubble constant

$$\tilde{h} = 0.65 \pm 0.15 \tag{10}$$

which is a compromise between measurements made by two groups: Tammann & Federspiel 1997 and Madore et al. 1998. We also employ nucleosynthesis constraints on the baryon density of

$$\widetilde{\Omega_b h^2} = 0.019 \pm 0.0024(95\%\mathrm{CL}) \tag{11}$$

given by Burles et al. 1999. An earlier value of $\widetilde{\Omega_b h^2} = 0.024 \pm 0.006$ by Tytler et al. 1996 will be used to analyze the influence of this assumption on the obtained cosmological parameters.

3. Testing the Method

In order to test our method to determine cosmological parameters for stability, we have constructed a mock sample of observational data. We start with a set of cosmological parameters and determine for them the "observational" data which would be measured in case of faultless measurements with 1σ errors comparable to the observational errors. We then insert random sets of starting parameters into the search program and try to find the right model which corresponds to the mock data. The method is stable if we can recover our input cosmological model. Even starting very far away from the true values, our method reveals as very stable and finds the 'true' model whenever possible (see Table 3).

One of the main ingredients for the solution for our search problem is a reasonably fast and accurate determination of the transfer function which depends on the cosmological parameters. We use the accurate analytical approximations of the MDM transfer function $T(k;z)$ depending on the parameters Ω_m, Ω_b, Ω_ν, N_ν and h by (Eisenstein & Hu 1999 and Novosyadlyj et al. 1999).

The linear power spectrum of matter density fluctuations is

$$P(k;z) = Ak^n T^2(k;z) D_1^2(z)/D_1^2(0), \tag{12}$$

where A is the normalization constant and $D_1(z)$ is the linear growth factor, which can be approximated by (Carroll, Press & Turner 1992)

$$D_1(z) = \frac{5}{2}\frac{\Omega_m(z)}{1+z}\left[\frac{1}{70} + \frac{209\Omega_m(z) - \Omega_m^2(z)}{140} + \Omega_m^{4/7}(z)\right]^{-1},$$

where $\Omega_m(z) = \Omega_m(1+z)^3/\left(\Omega_m(1+z)^3 + \Omega_\Lambda\right)$.

We normalize the spectra to the 4-year COBE data which determines the amplitude of density perturbation at the horizon crossing scale, δ_h (Liddle et al. 1996, Bunn and White 1997), which for a matter dominated Universe without tensor mode and cosmological constant is given by

$$\delta_h = 1.95 \times 10^{-5}\Omega_m^{-0.35-0.19\ln\Omega_m - 0.17\tilde{n}} e^{-\tilde{n}-0.14\tilde{n}^2}\ . \tag{13}$$

For a flat model with cosmological constant ($\Omega_m + \Omega_\Lambda = 1$) we have

$$\delta_h = 1.94 \times 10^{-5}\Omega_m^{-0.785-0.05\ln\Omega_m} e^{-0.95\tilde{n}-0.169\tilde{n}^2} \tag{14}$$

($\tilde{n} \equiv n - 1$). The normalization constant A is then given by

$$A = 2\pi^2\delta_h^2(3000/h)^{3+n}\ \mathrm{Mpc}^4. \tag{15}$$

The Abell-ACO power spectrum is related to the matter power spectrum at $z = 0$, $P(k;0)$ by the cluster biasing parameter b_{cl}. We assume scale-independent, linear bias:

$$P_{A+ACO}(k) = b_{cl}^2 P(k;0). \tag{16}$$

For a given set of parameters n, Ω_m, Ω_b, h, Ω_ν, N_ν and b_{cl} theoretical values of $P_{A+ACO}(k_j)$ can now be obtained for the values k_j of Table 1. We denote them by y_j ($j = 1, ..., 13$).

The dependence of the position and amplitude of the first acoustic peak of the CMB power spectrum on cosmological parameters has been investigated using CMBfast by Seljak & Zaldarriaga 1996. As expected, the results are, within sensible accuracy, independent of the hot dark matter contribution (Ω_ν). This is illustrated in Figs. 4 and 5. For the remaining parameters, n, h, Ω_b and Ω_Λ, we have

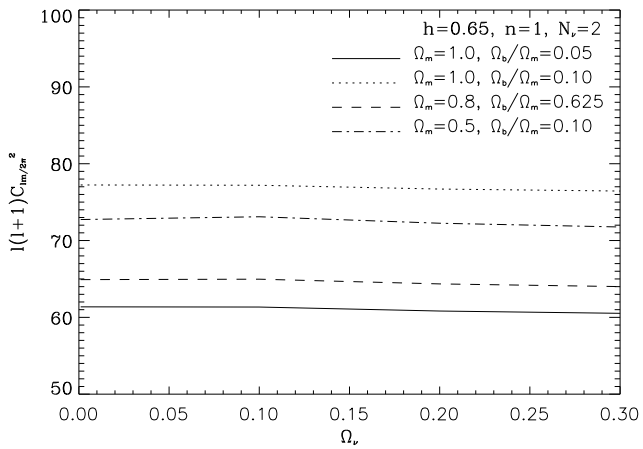

Fig. 4. The dependence of the acoustic peak amplitude A_p on neutrino content Ω_ν

determined the resulting values ℓ_p and A_p with CMBfast for a network of model parameters. The values ℓ_p, A_p in-between grid points are then obtained by 4-dimensional

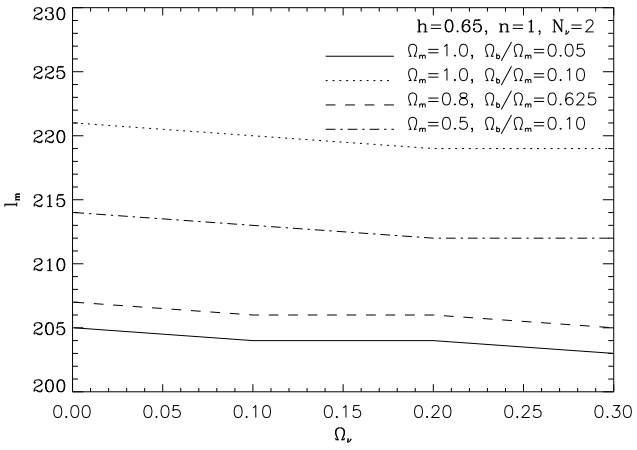

Fig. 5. The dependence of the acoustic peak position ℓ_p on neutrino content Ω_ν

interpolation. This allows a fast and sufficiently accurate calculation of the peak position and amplitude for a given set of parameters in the range $0.7 \leq n \leq 1.4$, $0.3 \leq h \leq 0.8$, $0 \leq \Omega_b \leq 0.2$ and $0 \leq \Omega_\Lambda \leq 0.8$ considered in this work. The accuracy of this interpolation is estimated to be within 2%. We denote ℓ_p and A_p by y_{14} and y_{15} respectively.

The theoretical values of the other experimental constraints are obtained as follows: The density fluctuation σ_8 is calculated according to Eq. (3) with $P(k;z)$ taken from Eq. (12). We set $y_{16} = \sigma_8 \Omega_m^{0.46-0.09\Omega_m}$ and $y_{17} = \sigma_8 \Omega^\alpha$, where $\alpha = 0.24$ for $\Omega_\Lambda = 0$ and $\alpha = 0.29$ for $\Omega_\Lambda > 0$, respectively.

The r.m.s. peculiar velocity of galaxies in a sphere of radius $R = 50h^{-1}$Mpc is given by

$$V_{50}^2 = \frac{1}{2\pi^2} \int_0^\infty k^2 P^{(v)}(k) e^{-k^2 R_f^2} W^2(50\text{Mpc } k/h) dk, \quad (17)$$

where $P^{(v)}(k)$ is power spectrum for the velocity field of the density-weighted matter (Eisenstein & Hu 1999), $W(50\text{Mpc } k/h)$ is the top-hat window function. A previous smoothing of raw data with a Gaussian filter of radius $R_f = 12h^{-1}$Mpc is employed here similar to the procedure which has led to the observational value. For the scales of interest $P^{(v)}(k) \approx (\Omega^{0.6} H_0)^2 P(k;0)/k^2$. We denote the r.m.s. peculiar velocity by y_{18}.

The value by Gnedin 1998 from the formation of Ly-α clouds constrains the r.m.s. linear density perturbation at $z = 3$ and $k_F = 38\Omega_m^{1/2} h$/Mpc. In terms of the power spectrum σ_F is given by

$$\sigma_F^2(z) = \frac{1}{2\pi^2} \int_0^\infty k^2 P(k;z) e^{(-k/k_F)^2} dk, . \quad (18)$$

It will be denoted by y_{19}. The corresponding value of the constraint by Croft et al. 1998 is

$$\Delta_\rho^2(k_p, z) \equiv k_p^3 P(k_p, z)/2\pi^2, \quad (19)$$

at $z = 2.5$ and $k_p = 0.008 H(z)/(1+z)(\text{km/s})^{-1}$, (where $H(z) = H_0 \left[\Omega_m (1+z)^3 + \Omega_\Lambda\right]^{1/2}$ is the Hubble parameter at redshift z) will be denoted by y_{20}. The slope of the power spectrum at this scale and redshift,

$$n(z) \equiv \frac{\Delta \log\ P(k,z)}{\Delta \log\ k}\ , \quad (20)$$

is denoted by y_{21}.

For all tests except Gnedin's Ly-α clouds we used the density weighted transfer function $T_{cb\nu}(k,z)$ from Eisenstein & Hu 1999. For Gnedin's σ_F we use $T_{cb}(k,z)$ according to the prescription of (Gnedin 1998). It must be noted that even in the model with maximal Ω_ν (~ 0.2) the difference between $T_{cb}(k,z)$ and $T_{cb\nu}(k,z)$ is less than 12% for $k \leq k_p$.

Finally, the values Ω_b and h are denoted by y_{22} and y_{23} respectively.

The relative quadratic deviations of the theoretical values from their observational counterparts are given by χ^2:

$$\chi^2 = \sum_{j=1}^{23} \left(\frac{\tilde{y}_j - y_j}{\Delta \tilde{y}_j} \right)^2, \quad (21)$$

where $\tilde{y}_j$ and $\Delta\tilde{y}_j$ are the experimental data and their dispersion, respectively. The set of parameters n, Ω_m, Ω_b, h, Ω_ν, N_ν and b_{cl} or some subset of them can be determined by minimizing χ^2 using the Levenberg-Marquardt method (Press et al. 1992). The derivatives of the predicted values with respect to the search parameters which are required by this method are calculated numerically using a relative step size of 10^{-5} with respect to the given parameter.

The method was tested in the following way. Assuming a 4-year COBE normalized tilted ΛMDM model with the parameters $n = 1.2$, $\Omega_m = 0.55$, $\Omega_b = 0.06$, $\Omega_\nu = 0.2$, $N_\nu = 2$, $h = 0.65$ and assuming further a cluster biasing parameter $b_{cl} = 3.0$ we have calculated mock cluster power spectrum $\tilde{P}_{A+ACO}(k_j)$ and treated them as $\tilde{y}_i$, $i = 1, ..., 13$. The remaining mock data $\tilde{y}_i$, $i = 14, ..., 23$ have been calculated as described above. We have assigned to these mock data the same relative 'experimental' errors as in the corresponding experiments described in the previous section.

We then used these mock data to search the parameters n, Ω_m, Ω_b, h, Ω_ν, and b_{cl} (N_ν was fixed). As starting parameters for the search program we assumed random values within the allowed range. We have searched for the parameters assuming the "true" value of two species of massive neutrinos as well as assuming three species of massive neutrinos. The parameters obtained for different cases are presented in Table 3. The errors in the determined parameters are calculated as root square from diagonal elements of the standard error covariance matrix. In all cases the code found all the previous known parameters with high accuracy. This means that the code finds the global minimum of χ^2 independent of the initial values for the parameters.

Table 3. Test of the method: results of parameter search from mock data for the tilted ΛMDM model ($n = 1.2$, $\Omega_m = 0.55$, $\Omega_b = 0.06$, $\Omega_\nu = 0.20$, $N_\nu = 2$, $h = 0.65$). In test 1, all parameters are determined; in the 2nd to 6th tests, some parameters are fixed. For each test the first row corresponds to the case when number of species of massive neutrinos is equal the input value (2) and the second - when $N_\nu = 3$.

No	N_ν	χ^2_{min}	n	Ω_m	Ω_ν	Ω_b	h	b_{cl}
1	2	0.00	1.20±0.07	0.55±0.15	0.200±0.059	0.060±0.022	0.65±0.12	3.00±0.45
	3	0.05	1.21±0.07	0.63±0.17	0.251±0.073	0.061±0.022	0.65±0.12	3.12±0.46
2	2	1.72	1.18±0.06	0.79±0.07	0.281±0.055	0.101±0.005	0.50*)	3.58±0.32
	3	3.84	1.21±0.06	0.98±0.08	0.446±0.035	0.101±0.005	0.50*)	3.65±0.30
3	2	0.00	1.20±0.07	0.55±0.05	0.200±0.036	0.060±0.003	0.65*)	3.00±0.27
	3	0.05	1.21±0.07	0.62±0.05	0.249±0.043	0.060±0.003	0.65*)	3.10±0.27
4	2	0.68	1.21±0.07	0.45±0.04	0.168±0.029	0.045±0.002	0.75*)	2.73±0.24
	3	0.80	1.22±0.07	0.51±0.05	0.207±0.034	0.045±0.002	0.75*)	2.83±0.25
5	2	0.00	1.20±0.07	0.55±0.05	0.200±0.036	0.060*)	0.65*)	3.00±0.27
	3	0.05	1.21±0.07	0.62±0.05	0.249±0.043	0.060*)	0.65*)	3.10±0.27
6	2	18.97	1.09±0.06	0.30*)	0.039±0.003	0.047±0.007	0.73±0.05	3.60±0.38
	3	18.20	1.02±0.08	0.30*)	0.000±0.001	0.064±0.021	0.63±0.10	3.55±0.31

(*) - fixed parameters.

Our conclusions from the test results can be summarized as follows:

1. If all parameters are free and $N_\nu = 2$ (the input value) the code finds the correct values of the free parameters (test 1, for $N_\nu = 2$ in Table 3).

2. If all parameters are free and $N_\nu = 3$ the code finds values of the free parameters which are in the 1σ range of errors (test 1, for $N_\nu = 3$ in Table 3).

3. If some parameters are fixed and differ from the input values (tests 2, 4, 6 in Table 3) the code finds for the remaining search parameters values close to the correct ones. The most stable and accurate value is Ω_b. The results for n, Ω_ν and Ω_m are in the $\leq 2\sigma$ range of the correct values. The most uncertain solutions are found for n and Ω_ν if an incorrect value for Ω_m has been assumed (test 6 in Table 3).

4. If some parameters are fixed to the predetermined ones and $N_\nu = 2$ (the input value) the code finds the correct values of the free parameters (test 3 and 5 , for $N_\nu = 2$ in Table 3), if $N_\nu = 3$ the determined values are within the 1σ range (test 3 and 5 , for $N_\nu = 3$ in Table 3).

In summary, the code determines the parameters n, Ω_ν, Ω_b, h, b_{cl} and Ω_m correctly, if the observational data are correctly measured and the cosmological model assumed is correct; *i.e.* no curvature, a negligible amount of tensor perturbations and a primordial spectrum of scalar perturbations which is scale free from the present horizon size down to the scale of the Ly-α clouds.

4. Results

The determination of the parameters n, Ω_m, Ω_b, h, Ω_ν, N_ν and b_{cl} by the Levenberg-Marquardt χ^2 minimization method can be realized in the following way: We vary the set of parameters n, Ω_m, Ω_b, h, Ω_ν and b_{cl} or some subset of them and find the minimum of χ^2. Since the N_ν process is discrete we repeat this procedure three times for N_ν=1, 2, and 3. The lowest of the three minimums is the minimum of χ^2 for the complete set of free parameters. The number of degrees of freedom $N_F = N_{\rm exp} - N_{\rm par} = 7$ if all parameters are free. It increases, if some of the parameters are fixed to a certain value. (Remember that even though we have 13 power spectra points, they can be described by just 3 degrees of freedom.)

We have determined the minimum of χ^2 for N_ν=1, 2, 3 in 11 different cases, where all observational data described in Sect. 2 are used.

1) n, Ω_m, Ω_ν, Ω_b, h, and b_{cl} are free parameters ($N_F = 7$);

2) $h = 0.5$ is fixed, the remaining parameters are free ($N_F = 8$);

3) $h = 0.6$ (Saha et al. 1999,Tammann et al. 1999) is fixed, the remaining parameters are free ($N_F = 8$);

4) $h = 0.72$ (Madore et al. 1998, Richtler et al. 1999) is fixed, the remaining parameters are free ($N_F = 8$);

5) $h = 0.6$ (Saha et al. 1999,Tammann et al. 1999) and $h^2\Omega_b = 0.024$ (Tytler et al. 1996) are fixed, the remaining parameters are free ($N_F = 9$);

6) $\Omega_m = 1.0$ is fixed, the remaining parameters are free ($N_F = 8$);

7) $\Omega_m = 0.3$ is fixed, the remaining parameters are free ($N_F = 8$);

8) $n = 1$ is fixed, the remaining parameters are free ($N_F = 8$);

9) $n = 1$, $\Omega_m = 1$ are fixed, the remaining parameters are free ($N_F = 9$);

10) $n = 1$, $\Omega_m = 0.3$ and are fixed, the remaining parameters are free ($N_F = 9$);

11) $\Omega_\nu = 7.4 \times 10^{-4} N_\nu / h^2$ is fixed by the lower limit of neutrino mass inferred by the observed neutrino oscillations in the Super-Kamiokande experiment ($N_F = 8$).

For these 11 cases we find the minimum of χ^2 from which we determine the parameters presented in Table 4. Note, that for all models χ^2_{min} is in the range, $N_F - \sqrt{2N_F} \leq \chi^2_{\rm min} \leq N_F + \sqrt{2N_F}$ which is expected for a Gaussian distribution of N_F degrees of freedom. This means that the cosmological paradigm which has been assumed is in agreement with the data. (Note here, that the reduction of the 13 not independent data points of the cluster power spectrum to three parameters is very important for our analysis. Otherwise we would obtain a $\chi_{\rm min}$ which is by far too small. If we would have assumed the 13 points of the Abell cluster power spectrum as independent, resulting in $N_F = 17$, the smallness of $\chi_{\rm min}$ would have indicated that something is wrong in our approach. But we might have drawn the wrong conclusion that the error bars be too large!) In Table 5 we present also the values of the different observational constraints for the best fit models found in Table 4.

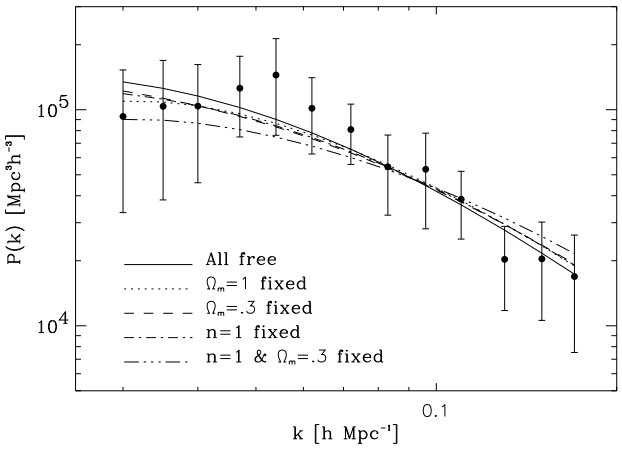

Fig. 6. The observed Abell-ACO power spectrum (filled circles) and the theoretical spectra predicted by tilted ΛMDM models with parameters taken from Table 4 ($N_\nu = 1$).

If all parameters are free (Table 4, case No 1), the model with one sort of massive neutrinos provides the best fit to the data, $\chi^2_{min} \approx 4.6$. Note, however, that there are only marginal differences in χ^2_{min} for $N_\nu = 1, 2, 3$. Therefore, with the given accuracy of the data we cannot conclude whether – if massive neutrinos are present at all – their number is one, two, or three. We summarize, that the considered observational data on LSS of the Universe can be explained by a flat ΛMDM inflationary model with a tilted spectrum of scalar perturbations and vanishing tensor contribution. The best fit parameters are: $n = 1.12 \pm 0.10$, $\Omega_m = 0.41 \pm 0.11$, $\Omega_\nu = 0.059 \pm 0.028$, $N_\nu = 1$, $\Omega_b = 0.039 \pm 0.014$ and $h = 0.70 \pm 0.12$. The CDM density parameter is $\Omega_{cdm} = 0.31 \pm 0.15$ and Ω_Λ is considerable, $\Omega_\Lambda = 0.59 \pm 0.11$.

The value of the Hubble constant is close to measurements by Madore et al. 1998. The spectral index coincides with the COBE prediction. The neutrino matter density $\Omega_\nu = 0.059 \pm 0.028$ corresponds to a neutrino mass $m_\nu = 94 \Omega_\nu h^2 \approx 2.7 \pm 1.2$ eV. The estimated cluster bias parameter $b_{cl} = 2.23 \pm 0.33$ fixes the amplitude of the Abell-ACO power spectrum (Fig. 6). All predictions of the measurements summarized in Table 5 are close to the experimental values and within the error bars of the data.

The predicted position of the acoustic peak ($\ell_p = 215$) is systematically lower than the experimental value determined here from the complete data set on $\Delta T/T$ ($\tilde{\ell}_p = 253 \pm 70$). This position is nearly fixed by the requirement $\Omega_m + \Omega_\Lambda = 1$ and is only weakly dependent of the parameters varied in this study. The acoustic peak inferred by the Boomerang experiment (Mauskopf et al. 1999) is situated at $\ell \sim 200$ and prefers models which are very close to flat (Melchiorri et al. 1999b). The models with low $\Omega_m \sim 0.3$ (case No. 7 in Table 4) fit the observable data somewhat less good than the best model ($\Delta\chi^2_{min} \approx 2.0$) but all predictions are still within the 1σ range. These models prefer a high Hubble parameter, $h \approx 0.7$ and no massive neutrinos, $\Omega_\nu = 0$. On the contrary, the matter dominated tilted MDM model ($\Omega_m = 1$, models 6 in Table 4) prefers high $\Omega_\nu = 0.22$, three sort of massive neutrino and a low Hubble parameter, $h = 0.47$. This can be understood by considering one of the most serious problems of standard CDM, namely that the model, when normalized to COBE, has too much power on small scales. This problem can be solved either by introducing HDM and thereby damping the spectrum on small scales or by introducing a cosmological constant which leads mainly to a 'shift of the power spectrum to the left'.

Another interesting correlation can be seen in Table 4, cases No 2-4, where we have fixed h. An increasing Hubble constant is compensated by a decreasing matter density, Ω_m, (*i.e.* increasing cosmological constant) and a decreasing baryon content due to the tight nucleosynthesis constraint on $\Omega_b h^2$. Furthermore, increasing the number of massive neutrino species N_ν from 1 to 3 leads to an increase of Ω_ν from 0.06 to 0.13 and to a decrease of Ω_Λ from 0.59 to 0.43 (case 1).

Table 4. Cosmological parameters determined for the tilted ΛMDM model with one, two and three species of massive neutrinos. In case No. 1 all parameters are free, in the other cases (No2-11) some of them are fixed, as described above.

No	N_ν	χ^2_{min}	n	Ω_m	Ω_ν	Ω_b	h	b_{cl}
1	1	4.64	1.12±0.09	0.41±0.11	0.059±0.028	0.039±0.014	0.70±0.12	2.23±0.33
	2	4.82	1.13±0.10	0.49±0.13	0.103±0.042	0.039±0.014	0.70±0.13	2.33±0.36
	3	5.09	1.13±0.10	0.56±0.14	0.132±0.053	0.040±0.015	0.69±0.13	2.45±0.37
2	1	7.50	1.11±0.09	0.64±0.10	0.075±0.058	0.076±0.005	0.50*)	2.72±0.28
	2	7.46	1.12±0.09	0.73±0.12	0.120±0.075	0.076±0.005	0.50*)	2.86±0.28
	3	7.46	1.13±0.09	0.82±0.14	0.163±0.089	0.076±0.005	0.50*)	2.96±0.29
3	1	5.28	1.12±0.09	0.51±0.07	0.074±0.041	0.053±0.003	0.60*)	2.43±0.26
	2	5.45	1.13±0.09	0.59±0.08	0.110±0.053	0.053±0.003	0.60*)	2.56±0.26
	3	5.62	1.13±0.09	0.66±0.10	0.144±0.063	0.053±0.003	0.60*)	2.66±0.27
4	1	4.67	1.12±0.10	0.39±0.05	0.058±0.026	0.037±0.002	0.72*)	2.19±0.23
	2	4.84	1.13±0.06	0.47±0.06	0.101±0.014	0.037±0.002	0.72*)	2.29±0.18
	3	5.12	1.14±0.10	0.53±0.07	0.130±0.046	0.037±0.002	0.72*)	2.38±0.25
5	1	5.68	1.11±0.09	0.53±0.07	0.068±0.043	0.067*)	0.60*)	2.49±0.27
	2	5.76	1.11±0.09	0.61±0.09	0.103±0.056	0.067*)	0.60*)	2.62±0.27
	3	5.85	1.12±0.09	0.67±0.10	0.136±0.067	0.067*)	0.60*)	2.71±0.27
6	1	12.23	1.07±0.09	1.00*)	0.116±0.086	0.118±0.027	0.40±0.05	3.15±0.39
	2	10.18	1.10±0.09	1.00*)	0.177±0.086	0.099±0.022	0.44±0.05	3.10±0.38
	3	8.80	1.12±0.09	1.00*)	0.219±0.084	0.085±0.019	0.47±0.05	3.07±0.38
7	1	6.55	1.04±0.10	0.30*)	0.000±0.005	0.038±0.013	0.71±0.12	2.25±0.19
	2	6.55	1.04±0.10	0.30*)	0.000±0.005	0.038±0.013	0.71±0.12	2.25±0.19
	3	6.55	1.04±0.10	0.30*)	0.000±0.005	0.038±0.013	0.71±0.12	2.25±0.19
8	1	6.21	1.00*)	0.45±0.12	0.042±0.033	0.038±0.014	0.71±0.13	2.44±0.31
	2	6.60	1.00*)	0.50±0.14	0.062±0.043	0.038±0.014	0.71±0.13	2.57±0.32
	3	6.85	1.00*)	0.51±0.14	0.063±0.012	0.038±0.014	0.71±0.13	2.69±0.32
9	1	13.01	1.00*)	1.00*)	0.088±0.075	0.104±0.027	0.43±0.05	3.23±0.36
	2	11.46	1.00*)	1.00*)	0.130±0.073	0.086±0.024	0.47±0.06	3.23±0.35
	3	10.46	1.00*)	1.00*)	0.159±0.069	0.075±0.021	0.51±0.07	3.23±0.35
10	1	6.94	1.00*)	0.30*)	0.000±0.010	0.034±0.009	0.75±0.09	2.25±0.20
	2	6.94	1.00*)	0.30*)	0.000±0.010	0.034±0.009	0.75±0.10	2.25±0.20
	3	6.94	1.00*)	0.30*)	0.000±0.010	0.034±0.009	0.75±0.10	2.25±0.20
11	1	6.34	1.04±0.07	0.35±0.10	0.002**)	0.045±0.016	0.65±0.11	2.36±0.26
	2	6.48	1.04±0.07	0.36±0.10	0.004**)	0.045±0.016	0.65±0.11	2.38±0.26
	3	6.63	1.04±0.07	0.37±0.10	0.005**)	0.046±0.016	0.64±0.11	2.41±0.26

*) - fixed parameters, **) mass density of neutrino is fixed by the lowest limit of the neutrino mass from Super-Kamiokande results, $h^2\Omega_\nu = \sqrt{\delta m^2} N_\nu / 94eV$ with $\sqrt{\delta m^2} = 0.07$eV.

If we use the nucleosynthesis constraint by Tytler et al. 1996 (case No 5), χ^2_{min} is slightly higher than in case No 3.

Now let us discuss models with a perfectly scale invariant primordial power spectrum as predicted by the first inflationary models, $n = 1$ fixed (cases 8-10 in Tables 4). If all of the remaining parameters are free (case 8) then this data set prefers a ΛMDM model with parameters $\Omega_m = 0.45 \pm 0.12$ and $h = 0.71 \pm 0.13$ and a somewhat lower neutrino content than the best fit model. Models with low matter content, $\Omega_m = 0.3$, prefer a high Hubble parameter, $h \simeq 0.75$ and no hot dark matter, $\Omega_\nu = 0$ (case No 10). The matter dominated model $\Omega_m = 1$ (case No 9) is the standard MDM model with $\Omega_\nu = 0.16 \pm 0.07$, three sort of massive neutrino ($m_\nu = 1.3 \pm 0.7$eV) and $h = 0.51 \pm 0.07$.

If the HDM component is eliminated or Ω_ν is fixed at the small value defined by the lower limit of the neutrino

Table 5. Theoretical predictions for the observational values of tilted ΛMDM models found with the parameters of Table 4 (for the value of N_ν leading to the lowest χ^2).

No	N_ν	ℓ_p	A_p	$\sigma_8\Omega_m^{0.46-0.09\Omega_m}$	$\sigma_8\Omega_m^{0.29}$	V_{50},km/s	σ_F	$\Delta_p^2(k_p)$	$n_p(k_p)$	$t_0/10^9$yrs
1	1	215	84.1	0.65	0.74	353	2.03	0.48	-2.28	12.3
2	1	233	91.6	0.68	0.71	348	1.87	0.51	-2.16	15.0
3	1	223	87.8	0.67	0.73	356	1.91	0.52	-2.18	13.5
4	1	214	83.2	0.65	0.74	353	2.04	0.49	-2.28	12.2
5	1	224	89.3	0.67	0.72	353	1.89	0.52	-2.18	13.3
6	3	228	84.7	0.72	0.72	366	1.78	0.44	-2.16	13.9
7	1	217	80.7	0.59	0.70	297	2.08	0.68	-2.17	13.4
8	1	209	69.5	0.65	0.72	323	1.88	0.58	-2.22	11.9
9	3	218	68.9	0.71	0.71	331	1.72	0.47	-2.21	12.8
10	1	213	73.4	0.59	0.70	292	2.00	0.67	-2.20	12.5
11	1	221	80.9	0.62	0.71	300	2.03	0.65	-2.18	14.1
Obs.	data	253 ± 70	80 ± 17	0.60 ± 0.08	0.8 ± 0.1	375 ± 85	$2.0 \pm .3$	0.57 ± 0.26	-2.25 ± 0.2	13.2 ± 3

mass $\sqrt{\delta m_\nu^2} = 0.07$ from the Super-Kamiokande experiment $\Omega_\nu = 7.4 \times 10^{-4} N_\nu/h^2$, we obtain the best-fit value for the matter density parameter $\Omega_m \approx 0.39 \pm 0.11$ and Hubble constant $h = 0.62 \pm 0.12$ (case No 11).

The experimental Abell-ACO power spectrum and the theoretical predictions for some best fit models are shown in Fig. 6. Recently it was shown (Novosyadlyj 1999) that due to the large error bars, the position of the peak of $\tilde{P}(k)$ at $k \approx 0.05$h/Mpc does not influence the determination of the cosmological parameters significantly. Mainly the slope of the power spectrum on scales smaller than the scale of the peak position determines the cosmological parameters.

The errors in the best fit parameters presented in Table 4 are the square roots of the diagonal elements of the covariance matrix. More informations about the accuracy of the determination of parameters and their sensitivity to the data used can be obtained from the contours of confidence levels presented in Fig. 7 for the tilted ΛMDM model with parameters from Table 4 (case No 1, $N_\nu = 1$). The same contours for cases No 6 and 7 are shown in Fig. 8 and 9, respectively. These contours show the confidence regions which contain 68.3% (solid line), 95.4% (dashed line) and 99.73% (dotted line) of the total probability distribution in the two dimensional sections of the six-dimensional parameter space, if the probability distribution is Gaussian. Since the number of degrees of freedom is 7 they correspond to $\Delta\chi^2$ =8.2, 14.3 and 21.8 respectively. The parameters not shown in a given diagram are set to their best-fit value.

As one can see in Fig.7a the iso-χ^2 surface is rather prolate from the low-Ω_m - high-n corner to high-Ω_m - low-n. This indicates some degeneracy in $n - \Omega_m$ parameter plane, which can be expressed by the following equation which roughly describes the 'maximum likelihood ridge' in this plane within the 1σ:

$$n\sqrt{\Omega_m} = 0.73\ . \tag{22}$$

A similar degeneracy is observed in the $\Omega_\nu - \Omega_m$ plane in the range $0 \le \Omega_\nu \le 0.17$, $0.25 \le \Omega_m \le 0.6$ (Fig.7c). The equation for the 'maximum likelihood ridge' or 'degeneracy equation' has here the form:

$$\Omega_\nu = 0.023 - 0.44\Omega_m + 1.3\Omega_m^2\ . \tag{23}$$

The 3rd column of Table 4 (χ^2_{min}) shows that all models except 9th with $N_\nu = 1$ are within the 1σ contour of the best fit.

The next important question is: which is the confidence limit of each parameter marginalized over the other ones. The straight forward answer is the integral of the likelihood function over the allowed range of all the other parameters. But for a 6-dimensional parameter space this is computationally time consuming. Therefore, we have estimated the 1σ confidence limits for all parameters in the following way. By variation of all parameter we determine the 6-dimensional χ^2 surface which contains 68.3% of the total probability distribution. We then project the surface onto each axis of parameter space. Its shadow on the parameter axes gives us the 1σ confidence limits on

cosmological parameters. For the best ΛMDM model with one sort of massive neutrinos the 1σ confidence limits on parameters obtained in this way are presented in Table 6.

Table 6. The best fit values of all the parameters with errors obtain by maximizing the (Gaussian) 68% confidence contours over all other parameters.

parameter	central value and errors
Ω_m	$0.41^{+0.59}_{-0.22}$
Ω_ν	$0.06^{+0.11}_{-0.06}$
Ω_b	$0.039^{+0.09}_{-0.018}$
$h^{*)}$	$0.70^{+0.15(+0.31)}_{-0.32}$
n	$1.12^{+0.27}_{-0.30}$
b_{cl}	$2.22^{+1.3}_{-0.7}$

*) - the upper limit is obtained by including the lower limit on the age of the Universe due to the age of oldest stars, $t_0 \geq 13.2 \pm 3.0$ (Carretta et al. 1999). The value obtained without this constraint is given in parenthesis.

It must be noted that the upper 1σ edge for h is equal 1.08 when we marginalized over all other parameters and input observable data used here. But this contradicts the age of the oldest globular clusters $t_0 = 13.2 \pm 3.0$ (Carretta et al. 1999). Thus we have included this value into the marginalization procedure for the upper limit of h. We then have 8 degrees of freedom (24 data points) and the 6-dimensional χ^2 surface which contains 68.3% of the probability is confined by the value 13.95. We did not use the age of oldest globular cluster for searching of best fit parameters in general case because it is only a lower limit for age of the Universe, besides it does not change their values as one can see from last column of Table 5.

The errors given in Table 6 represent 68% likelihood, of course, only when the probability distribution is Gaussian. As one can see from Fig.7 (all panels without degeneracy) the ellipticity of the likelihood contours in most of planes is close to what is expected from a Gaussian distribution. This indicates that our estimates of the confidence limits are reasonable. These errors define the range of each parameter within which the best-fit values obtained for the remaining parameters lead to $\chi^2_{min} \leq 12.84$. Of course, the best-fit values of the remaining parameters lay within their corresponding 68% likelihood given in the Table 6. It does however not mean that any set of parameters from these ranges satisfies the condition, $\chi^2_{min} \leq 12.84$.

For example, standard CDM model ($\Omega_m = 1$, $h = 0.5$, $\Omega_b = 0.05$, $n = 1$ and best-fit value of cluster biasing parameter $b_{cl} = 2.17$ ($\sigma_8 = 1.2$)) has $\chi^2_{min} = 142$ (!), that excludes it at very high confidence level, $> 99.999\%$. When we use the baryons density inferred from nucleosynthesis ($h^2\Omega_b = 0.019$ ($b_{cl} = 2.25$, $\sigma_8 = 1.14$)) the situation does not improve much, $\chi^2_{min} = 112$. Furthermore, even if we leave h as free parameter we still find $\chi^2_{min} = 16$ ($> 1\sigma$) with the best-fit values $h = 0.37$ and $b_{cl} = 3.28$ ($\sigma_8 = 0.74$); this variant of CDM is ruled out again by direct measurements of the Hubble constant.

The standard MDM model ($\Omega_m = 1$, $h = 0.5$, $\Omega_b = 0.5$, $n = 1$, $\Omega_\nu = 0.2$, $N_\nu = 1$ with a best value of the cluster biasing parameter $b_{cl} = 2.74$ ($\sigma_8 = 0.83$)) does significantly better: it has $\chi^2_{min} = 23.1$ (99% C.L.) which is out of the 2σ confidence contour but inside 3σ. With the nucleosynthesis constraint the situation does not change: $\chi^2_{min} = 22$; also if we leave h as free parameter: $\chi^2_{min} = 21$, $h = 0.48$. But if, in addition, we let vary Ω_ν, we obtain $\chi^2_{min} = 13$ with best-fit values of $\Omega_\nu = 0.09$, $h = 0.43$, $b_{cl} = 3.2$ ($\sigma_8 = 0.73$). This means that the model is ruled out (as well as the model 9th in Table 4) by the data set considered in this work at $\sim 70\%$ confidence level only. But also here the best-fit value for h is very low. If we fix it at lower observational limit $h = 0.5$ then $\chi^2_{min} = 18.9$ (the best fit values are: $\Omega_\nu = 0.15$, $b_{cl} = 2.8$ ($\sigma_8 = 0.83$)), which corresponds to a confidence level of 95% .

Therefore, we conclude that the observational data set used here rules out CDM models with $h \geq 0.5$, a scale invariant primordial power spectrum ($n = 1$) and $\Omega_k = \Omega_\Lambda = 0$ at very high confidence level, $> 99.99\%$. MDM models with $h \geq 0.5$, $n = 1$ and $\Omega_k = \Omega_\Lambda = 0$ are ruled out at $\sim 95\%$ C.L.

The best-fit parameters for 31 models which are inside of 1σ range of the best model are presented in Table 4. We conclude also that the observational data set used here does not rule out any of the 32 models presented in Table 4 at high confidence level but defines the 1σ range of cosmological parameters for the ΛMDM models which match observations best.

One important question is how each point of the data influences our result. To estimate this we have excluded some data points from the searching procedure. We have determined the best-fit parameters for the cases:

- all points of Abell-ACO power spectrum $\tilde{P}_{A+ACO}(k_j)$ are excluded,
- data on position and amplitude of acoustic peak, $\tilde{\ell}_p$, $\tilde{A}_p$ are excluded,
- the value for σ_8 from Girardi et al. 1998, $\tilde{\sigma}_8\Omega_m^{0.46-0.09\Omega_m}$ is excluded,
- the value for σ_8 from Bahcall & Fan 1998, $\tilde{\sigma}_8\Omega_m^{0.29}$ is excluded,
- both these tests are excluded,
- the bulk motion, $\tilde{V}_{50}$, is excluded,
- the Ly-α constraint by Gnedin 1998 $\tilde{\sigma}_F(z = 3)$ is excluded,

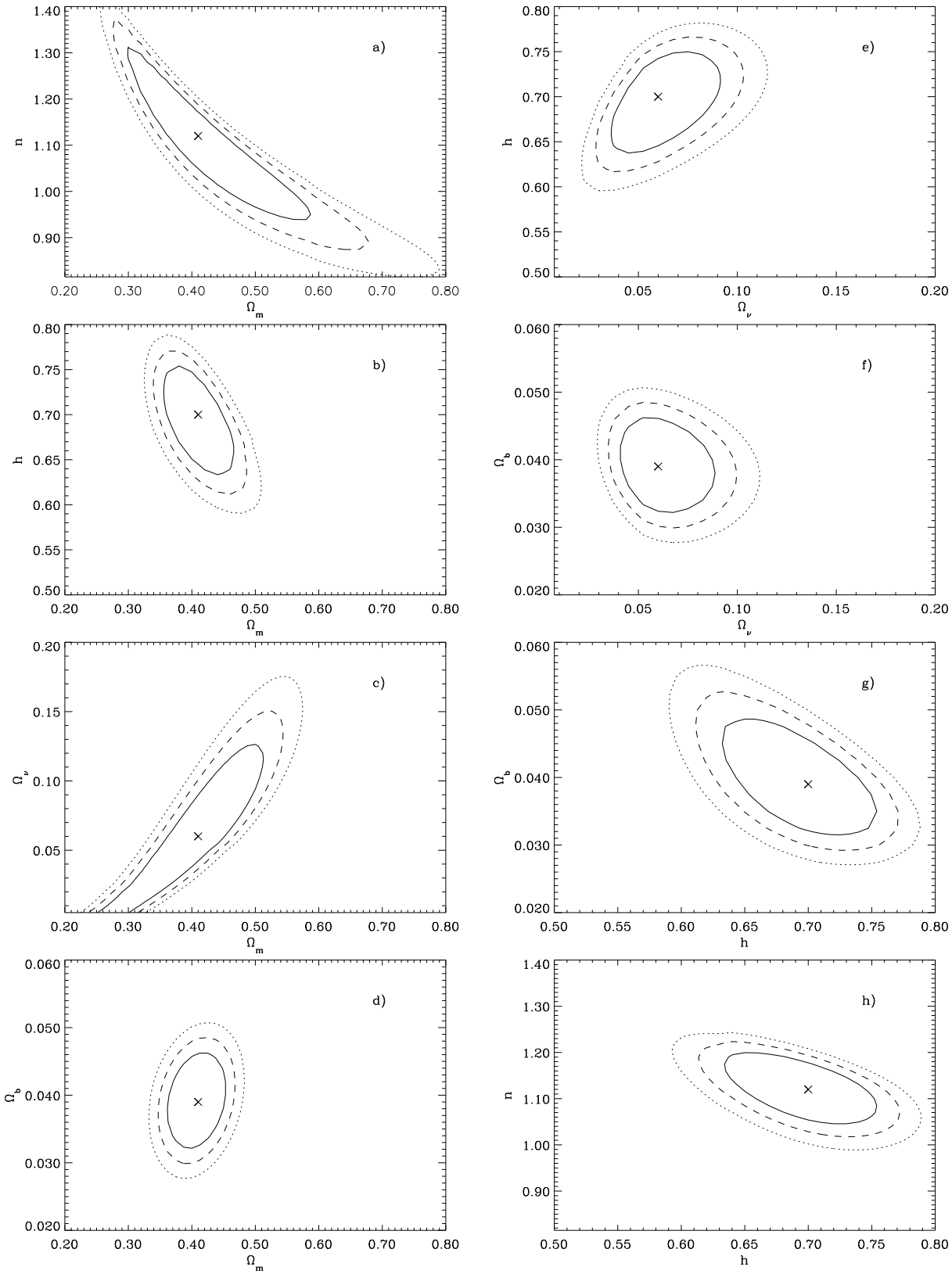

Fig. 7. Likelihood contours (solid line - 68.3%, dashed - 95.4%, dotted - 99.73%) of the tilted ΛMDM model with $N_\nu = 1$ and parameters from Table 4 (case 1) in the different planes of $n - \Omega_m - \Omega_\nu - \Omega_b - h$ space. The parameters not shown in a given diagram are set to their best fit value.

Table 7. Parameters determined for the tilted ΛMDM with one sort of massive neutrinos if some of the data are excluded from the searching procedure.

Excluded data	χ^2_{min}	n	Ω_m	Ω_ν	Ω_b	h	b_{cl}
All points of $\tilde{P}_{A+ACO}(k_j)$	1.45	1.10±0.08	0.42±0.11	0.053±0.021	0.041±0.013	0.68±0.11	****
$\tilde{\ell}_p$, $\tilde{A}_p$	4.22	1.15±0.15	0.40±0.11	0.065±0.033	0.040±0.016	0.69±0.14	2.20±0.33
$\tilde{\sigma}_8\tilde{\Omega}_m^{0.46-0.09\Omega_m}$	3.68	1.12±0.09	0.47±0.15	0.077±0.036	0.042±0.016	0.67±0.13	2.19±0.33
$\tilde{\sigma}_8\tilde{\Omega}_m^{0.29}$	4.03	1.11±0.10	0.40±0.11	0.052±0.031	0.041±0.015	0.68±0.12	2.32±0.35
Both σ_8 tests	3.65	1.12±0.10	0.46±0.17	0.072±0.048	0.042±0.016	0.67±0.13	2.22±0.38
$\tilde{V}_{50}$	4.57	1.11±0.10	0.41±0.11	0.057±0.030	0.039±0.014	0.70±0.12	2.25±0.34
$\tilde{\sigma}_F(z=3)$	4.61	1.13±0.11	0.39±0.12	0.056±0.030	0.038±0.014	0.71±0.13	2.19±0.36
$\tilde{\Delta}^2_\rho(k_p, z=2.5)$,$\tilde{n}_p(k_p, z=2.5)$	4.41	1.13±0.10	0.41±0.11	0.069±0.035	0.038±0.014	0.70±0.13	2.19±0.36
Both Lyα tests	3.70	1.11±0.10	0.56±0.22	0.222±0.291	0.042±0.017	0.67±0.13	2.27±0.40
$\tilde{h}$	4.28	1.11±0.10	0.35±0.13	0.051±0.024	0.030±0.017	0.79±0.22	2.11±0.39
$\tilde{\Omega}_b h^2$	4.04	1.14±0.09	0.37±0.10	0.068±0.017	0.000±0.000	0.66±0.10	2.14±0.33

– the Ly-α constraint by Croft et al. 1998 $\tilde{\Delta}^2_\rho(k_p, z = 2.5)$ and $\tilde{n}_p(k_p, z = 2.5)$ are excluded,
– both Ly-α tests are excluded,
– data on the direct measurements of Hubble constant $\tilde{h}$ is excluded, and
– the nucleosynthesis constraint by Burles et al. 1999 is not used.

The results for models with $N_\nu = 1$ and all parameters free are presented in Table 7 (see for comparison model 1 for $N_\nu = 1$ in Table 4). Excluding any part of observable data results only in a change of the best-fit values of n, Ω_m and h within the range of their corresponding standard errors. This indicates that the data are mutually in agreement, implying the same cosmological parameters (within the still considerable error bars). The small scale constraints, the Ly-α tests reduce the hot dark matter content from $\Omega_\nu \sim 0.22$ to ~ 0.075. The σ_8-tests further reduce Ω_ν to ~ 0.06. Including of the Abell-ACO power spectrum in the search procedure, tends to enhance Ω_ν slightly. The most crucial test for the baryon content is of course the nucleosynthesis constraint. Its $\sim 6\% - 1\sigma$-accuracy safely keeps $h^2\Omega_b$ near its median value 0.019. The parameter Ω_b in turn is only known to $\sim 36\%$ accuracy due to the large errors of other experimental data used here, especially Hubble constant. The obtained accuracy of h ($\sim 17\%$) is better than the one assumed from direct measurements, $\sim 23\%$. Summarizing, we conclude that all data points used here are important for searching the best-fit cosmological parameters.

5. Discussion

The best-fit parameters obtained in this paper are within the allowed range of parameters found by other authors using different constraints. For example, for the ΛMDM model with scale-invariant primordial power spectrum and one sort of massive neutrinos which contributes 10–20% of matter density, Valdarnini et al. 1998 found $0.45 \leq \Omega_m \leq 0.75$ for $h = 0.5$, and $0.3 \leq \Omega_m \leq 0.5$ for $h = 0.7$. Similar constraints have been given by Primack & Gross 1998 for ΛMDM models with two species of massive neutrinos. Our values of Ω_m are within these ranges. But at the boundary of this parameter range $\chi^2 \geq 20$, which is outside of the 2σ confidence contour.

Recently Bahcall et al. 1999 have shown that the CMB anisotropy data, the cluster evolution and the SNIa magnitude-redshift relation indicate a flat Universe with accelerated expansion, compatible with a $\Omega_\Lambda \simeq 0.7$ and $\Omega_m \approx 0.3$ if CDM ($\Omega_\nu = 0$) is assumed. As we can see from Table 4 (case No 11, 1), our analysis leads to the same conclusion if we set density of hot dark matter to the minimum value compatible with the Super-Kamiokande experiment (less than 1% of the total density). However, if Ω_ν is a free parameter, the observational data considered in this work lead to a ΛMDM with a slightly blue spectrum of primordial fluctuations (case No 1 in Table 4).

In our preferred tilted ΛMDM models (case No 1) the masses of neutrinos are $m_\nu = 2.7 \pm 1.2$ eV for model with $N_\nu = 1$, $m_\nu = 2.4 \pm 1.0$ eV when $N_\nu = 2$ and $m_\nu = 2.0 \pm 0.8$ eV for model with $N_\nu = 3$. The accuracy of neutrino mass or density determination is modest because the observational constraints depend stronger on Ω_m and n than on Ω_ν and N_ν. In models with fixed low matter density $\Omega_m = 0.3$ (case No 7 and 10) the best-fit values of the neutrino density are $\Omega_\nu \approx 0$, i.e. even below the lower limit of the massive neutrino contribution to the cosmological density indicated by the Super-Kamiokande experiment. However, the 1σ contours of the low Ω models include the Super-Kamiokande limit (see Fig. 9b).

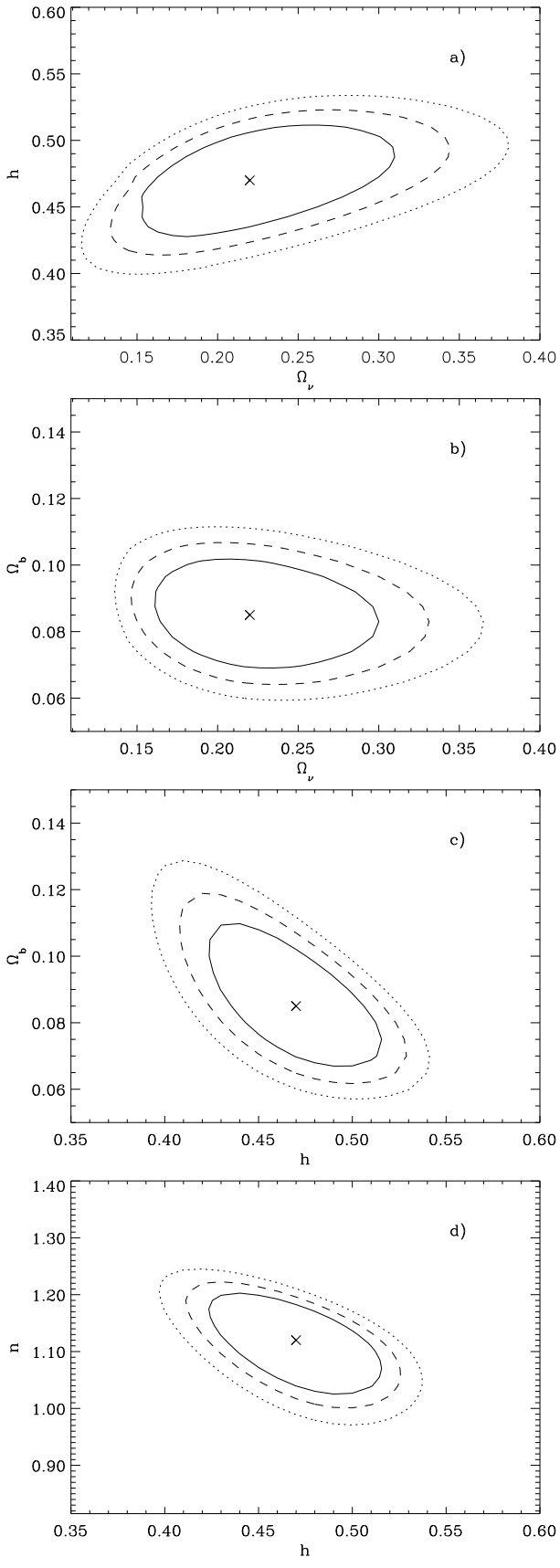

Fig. 8. Likelihood contours (solid line - 68.3%, dashed - 95.4%, dotted - 99.73%) of tilted ΛMDM with $N_\nu = 3$, fixed $\Omega_m = 1$ and parameters from Table 4 (case 6) in the different planes of $n - \Omega_\nu - \Omega_b - h$ space. The parameters not shown in a given

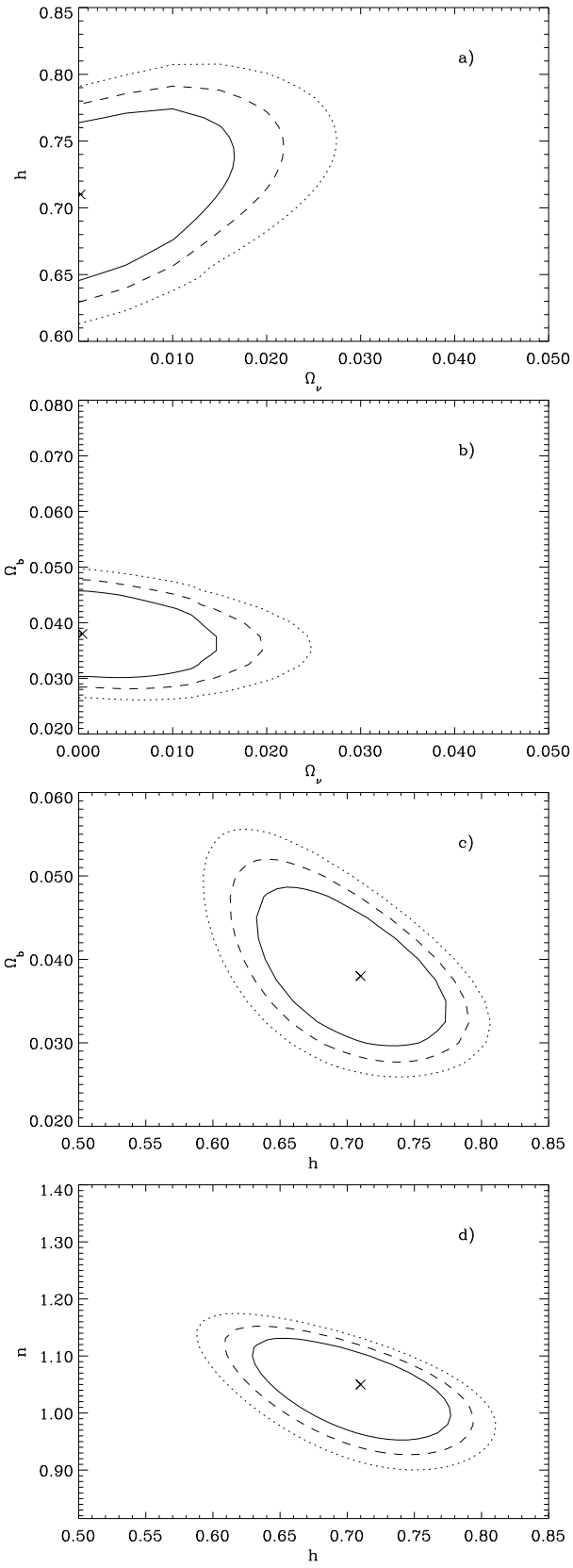

Fig. 9. Likelihood contours (solid line - 68.3%, dashed - 95.4%, dotted - 99.73%) of tilted ΛMDM with $N_\nu = 3$, fixed $\Omega_m = 0.3$ and parameters from Table 4 (case 7) in the different planes of $n - \Omega_\nu - \Omega_b - h$ space. The parameters not shown in a given diagram are set to their best fit value.

In the last column of Table 5 we also indicate the age of the Universe,

$$t_0 = \frac{2}{3H_0}\left[\frac{1}{2\Omega_\Lambda^{1/2}}\ln\frac{1+\Omega_\Lambda^{1/2}}{1-\Omega_\Lambda^{1/2}}\right], \quad (24)$$

for each model as well as the age of the oldest globular clusters (Carretta et al. 1999). All models with parameters taken from Table 4 have ages which are in agreement with the oldest objects of our galaxy.

We have used a scale independent, linear bias factor b_{cl} as free parameter in order to fit the Abell-ACO power spectrum amplitude.

Let us discuss in more detail how the model predictions presented in Table 5 match each observable constraint separately. The predicted position of the acoustic peak for all models is lower than the one determined from the observational data set presented in Table 2 ($\ell_p = 253 \pm 70$). Tilted ΛMDM models prefer $\ell_p \sim 210 - 230$. This is due to the fact that the peak position depends only very weakly on the parameters discussed in this work. It is determined mainly by spatial curvature which we have set to zero here (together with the initial conditions which we have assumed to be adiabatic). However, our result is in good agreement with the most recent and so far most accurate determination of the peak position from one single experiment, the North American test flight of Boomerang (Mauskopf et al. 1999, Melchiorri et al. 1999b), which led to $0.85 \leq \Omega_m + \Omega_\Lambda \leq 1.25$ with maximum likelihood near 1 for adiabatic CDM models. The prediction of our best model for position of the first acoustic peak ($\ell = 215$) matches the value given by Boomerang experiment $\ell \sim 200$ very well. The central value from the combination of all available experiments, $\ell_p = 253$, may very well be contaminated by mutual calibration inconsistencies.

Finally we want to discuss the possibility of using the averaged power spectrum of galaxies obtained by Einasto et al. 1999 to determine the parameters. This averaged spectrum of galaxies is determined in a wide range of scales ($0.02h/\mathrm{Mpc} \leq k \leq 10h/\mathrm{Mpc}$) and has substantially lower errors than the Abell-ACO power spectrum used here. Its 1σ errors are $\sim 4\%$ on small scales and $\sim 20\%$ at large scales versus $\sim 40\%$ and $\sim 60\%$ respectively for the Abell-ACO power spectrum. It is interesting to compare the predictions obtained from the power spectrum of galaxies with our analysis, because, as already mentioned in the introduction, the correction of the linear power spectrum for nonlinear evolution must be included into the algorithm. We use the fitting function by Smith et al. 1997, which transfers the linear into the nonlinear power spectrum, and the observational constraint for the Hubble constant $\tilde{h} = 0.6 \pm 0.02$ (Saha et al. 1999,Tammann et al. 1999) as well as the nucleosynthesis constraint for the baryon content by Burles et al. 1999. Under these assumptions we find the following best fit parameters: $n = 1.11 \pm 0.02$, $h = 0.62 \pm 0.02$, $\Omega_m = 0.2 \pm 0.03$, $\Omega_b = 0.044 \pm 0.005$, $\Omega_\nu = 0.01 \pm 0.01$, $N_\nu = 3$ and galaxy biasing parameter $b_g = 1.52 \pm 0.06$.

If we add the remaining observations described in Sect.s 2.2 and 2.3 the best-fit parameters remain practically unchanged due to the large number of (probably not independent) data points in the galaxy power spectrum. A model with these parameters has serious problems reproducing the experimental data set used here. Indeed, with these parameters we obtain $\chi^2 \approx 61$, for the data set used in the rest of this work, far outside 3σ contour. The model predictions $\sigma_8 \Omega_m^{0.46-0.09\Omega_m} = 0.28$ and $\sigma_8 \Omega_m^{0.29} = 0.35$ are $\sim 4\sigma$ lower than the corresponding observational values by Girardi et al. 1998 and Bahcall & Fan 1998. Moreover, the peculiar velocity V_{50} is $\sim 2\sigma$ lower than the observed value, $\sigma_F(z = 3)$ is and $\Delta^2_\rho(k_p, z = 2.5)$ are $\sim 3\sigma$ and $\sim 1.5\sigma$ lower than the corresponding values inferred from the Ly-α measurements. Therefore, we conclude that a model with parameters determined by the galaxy power spectrum is ruled out by the observations discussed in this work.

This result is not completely unexpected, because the galaxy power spectrum on small scales is probably influenced by a scale dependent bias (see for example Kravtsov & Klypin 1999, Fig. 3) which is not taken into account here. Moreover, the fitting formula for nonlinear evolution at $k \geq 1$ h/Mpc may be incorrect. If we disregard the short wavelength part of galaxy power spectrum we find parameters close to those presented in Table 4.

6. Conclusions

Using Levenberg-Marquardt χ^2 minimization method we have determined the cosmological parameters of spatially flat, tilted ΛMDM models. We searched for a maximum of 6 parameters: the spectral index n, the matter content Ω_m ($\Omega_m + \Omega_\Lambda = 1$), the hot dark matter content Ω_ν, the baryon content Ω_b, the dimensionless Hubble constant h and the biasing parameter for rich clusters, b_{cl}. The experimental data set used in the search procedure included the Abell-ACO power spectrum (Retzlaff et al. 1998), the position and amplitude of the first acoustic peak in the angular power spectrum of CMB temperature fluctuations determined from the set of published measurements on different scales, the constraints for the density fluctuation amplitude σ_8 derived from the mass function of nearby and distant clusters (Girardi et al. 1998, Bahcall & Fan 1998), the mean peculiar velocity of galaxies in a sphere of radius $50h^{-1}$Mpc (Kolatt & Dekel 1997), the constraints on amplitude and tilt of the power spectra at small scales obtained from Ly-α clouds at z=2-3 (Gnedin 1998, Croft et al. 1998), the nucleosynthesis constraints (Tytler et al. 1996, Burles et al. 1999) and the COBE data (Bunn and White 1997) which is used to normalize the model power spectra.

We have considered one, two and three species of massive neutrinos. We have studied the influence of a reduc-

tion of the number of free parameters. In Table 4 we summarize the parameters which we have determined in 33 different cases. Based on the results presented in Table 4 we conclude:

- The tilted ΛMDM model with one sort of massive neutrinos and the best-fit parameters $n = 1.12 \pm 0.10$, $\Omega_m = 0.41 \pm 0.11, \Omega_\Lambda = 0.59 \pm 0.11, \Omega_\nu = 0.059 \pm 0.028$, $\Omega_b = 0.039 \pm 0.014$ and $h = 0.70 \pm 0.12$ (standard errors) matches the observational data set best. The 1σ (68.3%) confidence limits on each cosmological parameter, obtained by marginalizing over the other parameters, are $0.82 \leq n \leq 1.39$, $0.19 \leq \Omega_m \leq 1$, $0 \leq \Omega_\Lambda \leq 0.81$, $0 \leq \Omega_\nu \leq 0.17$, $0.021 \leq \Omega_b \leq 0.13$ and $0.38 \leq h \leq 0.85$.
- The degeneracies in the $n - \Omega_m$ and $\Omega_\nu - \Omega_m$ planes $n\sqrt{\Omega_m} = 0.73$ and $\Omega_\nu = 0.023 - 0.44\Omega_m + 1.3\Omega_m^2$ are revealed.
- For fixed Hubble constant h raising from 0.5 to 0.72, the best-fit value for Ω_m decreases from 0.63 to 0.39 for ΛMDM models with $N_\nu = 1$. For models with $N_\nu = 2$ and 3 the value of Ω_m raises by ~ 0.08 and ~ 0.15 respectively. The Ω_ν is higher for more species of massive neutrinos, ~ 0.06 for one sort and ~ 0.13 for three, and decreases slowly for growing h. The inclination of initial power spectrum n correlates somewhat with Ω_ν and grows slightly with h.
- Fixing a low Ω_m=0.3 a ΛCDM model without HDM matches the observational data set best. In this case the parameters are $h = 0.71 \pm 0.12$, $n = 1.04 \pm 0.10$ and $\Omega_b = 0.038 \pm 0.013$.
- For all models the biasing parameter b_{cl} of rich clusters is in the range 2.2-3.3, for the best model it equals 2.23 ± 0.33 (standard error). The 1σ (68.3%) confidence interval is $1.5 \leq b_{cl} \leq 3.5$.
- CDM models with $h \geq 0.5$, scale invariant primordial power spectrum $n = 1$ and $\Omega_\Lambda = \Omega_k = 0$ are ruled out at very high confidence level, $> 99.99\%$.
- Also pure MDM models are ruled out at $\sim 95\%$ C.L.

Finally, we note that the accuracy of present observational data on the large scale structure of the Universe is still too low to constrain the set of cosmological parameters sufficiently, but we believe that our work shows the potential of such studies, which search for parameters including data from different, often complementary observations. It is clear that with sufficiently accurate data, such a study may also reveal an inconsistency of model assumptions.

Acknowledgments This work is part of a project supported by the Swiss National Science Foundation (grant NSF 7IP050163). B.N. is also grateful to DAAD for financial support (Ref. 325) and AIP for hospitality. V.N.L. is grateful to INTAS support (97-1192).

References

Archipova, N.A., Lukash, V.N., Mikheeva, E.V., 1999, Gravitation & Cosmology, 5, Suppl. "Cosmoparticle Physics", 159
Atrio-Barandela, F. et al., 1997, Pis'ma Zh. Eksp. Teor. Fiz. 66, 373
Bahcall, N.A., Fan, X., 1998, ApJ 504, 1
Bahcall, N.A., Ostriker, J.P., Perlmutter, S., Steinhardt, P.J., 1999, Science 284, 1481
Bardeen, J.M., Bond, J.R., Kaiser, N., Szalay, A.S., 1986, ApJ 304, 15
Bartlett, J.G., Douspis, M., Blanchard, A., Le Dour, M., 1999, submitted to A&A, astro-ph/9903045
Bennett, C.L. et al., 1996, ApJ 464, L1.
Borgani, S. et al., 1999, ApJ, 527, 561
Bridle, S.L., et al., 1999, astro-ph/9903472
Bunn E.F., White M., 1997, ApJ 480, 6
Burles, S., Nollett, K.M., Truran, J.N., Turner, M.S., 1999, Phys.Rev.Lett. 82, 4176
Carretta, E., Gratton, R.C., Clementini, G., Fusi Pecci, F., 1999, ApJ (in print), astro-ph/9902086
Carroll, S.M., Press, W.H., Turner, E.L., 1992, ARA&A 30, 499
Coble, K. et al., 1999, astro-ph/9902195
Croft, R.A.C. et al., 1998, ApJ 495, 44
Da Costa, L.N. et al., 1994, ApJ 437, L1
De Bernardis, P., de Gasperis, G., Masi, S., Vittorio, N., 1994, ApJ 433, L1
De Oliveira-Costa, A. et al., 1998, ApJ 509, L77
Dodelson, S., Gates, E., Stebbins, A., 1996, ApJ 467, 10
Einasto, J. et al., 1997, Nature 385, 139
Einasto, J. et al., 1999, ApJ, 515, 441
Eisenstein, D.J., Hu, W., 1999, ApJ 511, 5
Eisenstein, D.J., Hu, W., Silk, J., Szalay, A.S., 1998, ApJ 494, L1
Femenia, B. et al., 1997, ApJ 498, 117
Fukuda, Y. et al., 1998, Phys. Rev. Lett. 81, 1562
Ganga, K, Page, L., Cheng, E.S., Meyer, S., 1994, ApJ 432, L15
Girardi, M. et al., 1998, ApJ 506, 45
Gnedin N.Y., 1998, MNRAS 299, 392
Gnedin N.Y., 1999, private communication
Gunderson, J.O. et al., 1995, ApJ 443, L57
Gutiérrez, C.M., et al., 1997, ApJ 480, L83
Hancock, S. et al., 1997, MNRAS 289, 505
Kofman, L.A., Starobinsky, A.A., 1985, SvA Lett. 9, 643
Kolatt, T., Dekel, A., 1997, ApJ 479, 592
Kravtsov, A.V., Klypin, A., 1999, ApJ 520, 437
Lahav, O., Rees, M.J., Lilje, P.B., Primack, J., 1991, MNRAS 251, 128
Landy, S.D. et al., 1996, ApJ 456, L1
Leitch, E.M. et al., 1998, ApJ, 518
Liddle, A.R., Lyth, D.H., Viana, P.T.P., White, M., 1996, MNRAS 282, 281
Lineweaver, C.A., Barbosa, D., 1998, ApJ 496, 624
Maddox, S.J., Efstathiou, G., Sutherland, W.J., 1996, MNRAS 283, 1227
Madore, B.F. et al., 1999, ApJ, 515, 2941
Masi, S. et al., 1996, ApJ 463, L47
Mauskopf, P. et al., 1999, astro-ph/9911444.

Melchiorri, A., Sazhin, M.V., Shulga, V.V., Vittorio, N., 1999, ApJ 518, 562.
Melchiorri A., et al., 1999, astro-ph/9911445.
Miller, A.D. et al., 1999, ApJL, 524, L1
Netterfield, C.B. et al., 1997, ApJ 474, 47
Novosyadlyj B., 1999, Journal of Physical Studies V.3, No1, 122
Novosyadlyj, B., Durrer, R., Lukash, V.N., 1999, A&A 347, 799 (astro-ph/9811262)
Park, C., Vogeley, M.C., Geller, M.J., Huchra, J.P., 1994, ApJ 431, 569
Peebles P.J.E, 1980, Large Scale Structure of the Universe, Princeton University Press
Perlmutter, S. et al., 1998, Nature 391, 51
Piccirillo, L., Calisse, P., 1993, ApJ 411, 529
Platt, S.R. et al., 1997, ApJ 475, L1
Press, W.H., Flannery, B.P., Teukolsky, S.A., Vettrling, W.T., 1992, Numerical recipes in FORTRAN. New York: Cambridge Univ.Press
Primack, J.R., Gross, M.A., 1999, published in the Proceedings of the Xth Rencontres de Blois, "The Birth of Galaxies", astro-ph/9810204
Retzlaff, J. et al., 1998, New Astronomy v.3, 631
Richtler, T., Drenkhahn, G., Gomez, M., Seggewiss, W., 1999, astro-ph/9905080
Ricotti, M., Gnedin, N.Y., Shull, J.M., 1999, astro-ph/9906413, 2000, ApJ, 534, May 1 (in press)
Riess, A. et al., 1998, AJ, 116, 1009
Saha A., Sandage A., Tammann G.A., Labhardt L., et al., 1999, ApJ, 522, 802
Saunders, W., Rowan-Robinson, M., Lawrence, A., 1992, MNRAS 258, 134
Scott, P.F.S. et al., 1996, ApJ 461, L1
Seljak U., Zaldarriaga M., 1996, ApJ 469, 437
Smith, C.C. et al., 1997, MNRAS 297, 910
Tadros H., Estathiou G., 1996, MNRAS 282, 1381
Tammann, G.A., Federspiel, M., 1997, in "The Extragalactic Distance Scale", (eds.) M. Livio, M. Donahue, N. Panagia (Cambridge: Cambridge Univ. Press)
Tammann, G.A., Sandage, A., Reindl, B., 1999, astro-ph/9904360, also available on the CD-ROM Proceedings of the 19th Texas Symposium on Relativistic Astrophysics and Cosmology, eds. J. Paul and P. Peter
Tanaka, S.T. et al., 1996, ApJ 468, L81
Tegmark, M., 1999, ApJ 514, L69
Tegmark, M.'s homepage at `http://www.sns.ias.edu/~max/`
Tegmark, M., Hamilton, A., 1997, astro-ph/9702019, in proccedings of the 18th Texas Symposium on Relativistics Astrophysics & Cosmology 1996, eds A V Olinto, J A Frieman & D N Schramm, 270 (World Scientific)
Tucker, G.S. et al., 1997, ApJ 475, L73
Tytler, D., Fan, X.M., Burles, S., 1996, Nature 381, 207
Valdarnini, R., Kahniashvili, T., Novosyadlyj, B., 1998, A&A 336, 11
Vogeley M., Park C., Geller M.J., Huchra J.P., 1992, ApJ 391, L5
Wilson G.W. et al., 1999, astro-ph/9902047.

This article was processed by the author using Springer-Verlag LaTeX A&A style file *L-AA* version 3.